Platinum−Silicon Four-Membered Rings of Two Different Structural Types

Lee M. Sanow, Minghui Chai, David B. McConnville, Kevin J. Galat, Richard S. Simons, Peter L. Rinaldi, Wiley J. Youngs, and Claire A. Tessier*

Department of Chemistry, University of Akron, Akron, Ohio 44325-3601

Received November 1, 1999

The synthesis and characterization of platinum−silicon four-membered rings of two different structural types is reported. The reaction of $Pt(PR_3)_3$ (R = Et or Pr) and $Si(Hex)H_3$ (Hex = *n*-hexyl) gives $[Pt(PR_3)_2SiH(Hex)]_2$ (R = Et, **1a**; R = Pr, **1b**) and $[(R_3P)Pt(\mu\text{-}Si(\mu\text{-}H)\text{-}(Hex)(Pt(PR_3)_2)H)]_2$ (R = Et, **2a**; R = Pr, **2b**). The ratio of **1a** to **2a** is highly dependent on the reaction conditions, whereas **1b** is always the major product in the PPr_3 substituted case. Evidence that suggests that **1a** and **1b** are precursors to **2a** and **2b**, respectively, is presented. X-ray crystallography of the rings **1b** and **2a** shows they contain short Si−Si and Pt−Pt contacts, respectively. The ^{29}Si NMR chemical shifts for the two types of rings differ by over 250 ppm. A 2D-NMR study of these rings has provided detailed coupling information, including information on the agostic Pt−H−Si hydride in **2a**.

Introduction

Since its onset in 1941, the study of transition-metal silyl compounds has proven to be an important area of chemical research.[1] The discovery of their extensive laboratory and industrial applications in 1965 spurred the development of metal−silyl compounds, particularly their use as catalysts for hydrosilylation, dehydrogenative coupling, redistribution on silicon, and silicon−carbon bond-forming reactions.[1,2] Many of these reactions result in the formation of metal−silicon rings, a topic that has been reviewed.[3] Platinum−silicon rings were first mentioned in the early 1970s.[4] Since then, a number of three-[5] and four-membered[6−11] platinum−silicon rings have been reported.

Several different platinum−silicon frameworks have been firmly established for the four-membered rings. Rings of structure **1** are characterized by Si−Si distances that are within the range of known Si−Si bond lengths (2.55−2.65 Å), acute Si−Pt−Si angles (64−67°), and nonbonding Pt−Pt separations (3.97−4.00 Å).[7,9−11] Though two bonding studies indicate this short Si−Si distance represents a bonding interaction,[12,13] this interpretation is not universally accepted. Rings of structure **2** are characterized by a short Pt−Pt distance (2.708(1) Å) and an obtuse Si−Pt−Si angle (110°), both consistent with a Pt−Pt bond.[6,10] Ring **2** also contains two agostic Pt−H−Si moieties. A palladium analogue of **2** has recently been reported (Si−Pd−Si = 110°).[14]

Ring **3** might appear to be a variant of structure **1** because of its acute Si−Pt−Si angle (67°) and its short Si−Si distance of 2.720 Å, which is just marginally outside the range of known Si−Si bonds (2.30−2.70

* Corresponding author. E-mail: tessier@chemistry.uakron.edu.

(1) (a) Corey, J. Y.; Braddock-Wilking, J. *Chem. Rev.* **1999**, *99*, 175−292. (b) Eisen, M. S. In *The Chemistry of Organic Silicon Compounds*, Volume 2; Rappoport, Z., Apeloig, Y., Eds.; John Wiley & Sons: New York, 1998; Part 3, Chapter 35.

(2) (a) Gauvin, F.; Harrod, J. F.; Woo, H. G. *Adv. Organomet. Chem.* **1998**, *42*, 363−405. (b) Ojima, I.; Li, Z.; Zhu, J. In *The Chemistry of Organic Silicon Compounds*; Rappoport, Z., Apeloig, Y., Eds.; John Wiley & Sons: New York, 1998; Vol. 2, Part 2, Chapter 29. (c) Tilley, T. D. In *The Silicon-Heteroatom Bond*; Patai, S., Pappoport, Z., Eds.; Wiley & Sons: New York, 1991; Chapter 9. (d) Reichl, J. A.; Berry, D. H. *Adv. Organomet. Chem.* **1999**, *43*, 197−265. (e) Recatto, C. A. *Aldrich Chim. Acta* **1995**, *28*, 85−92. (f) Yamashita, H.; Tanaka, M. *Bull. Chem. Soc. Jpn.* **1995**, *68*, 403−419.

(3) (a) Ogino, H.; Tobita, H. *Adv. Organomet. Chem.* **1998**, *42*, 223−290. (b) Lickiss, P. D. *Chem Soc. Rev.* **1992**, *21*, 271−279. (c) Zybill, C. *Top. Curr. Chem.* **1991**, *160*, 1−45.

(4) (a) Chatt, J.; Eaborn, C.; Kapoor, P. N. *J. Chem. Soc. A* **1970**, 881−884. (b) Fink, W.; Wenger, A. *Helv. Chim. Acta* **1971**, *54*, 2186−2189.

(5) (a) Cirano, M.; Howard, J. A. K.; Spencer, J. L.; Stone, F. G. A.; Wadepohl, H. *J. Chem. Soc., Dalton Trans.* **1979**, 1749−1756. (b) Pham, E. K.; West, R. *J. Am. Chem. Soc.* **1989**, *111*, 7667. (c) Pham, E. K.; West, R. *Organometallics* **1990**, *9*, 1517−1523. (d) Pham, E. K.; West, R. *J. Am. Chem. Soc.* **1996**, *118*, 7871. (e) Brittingham, K. A.; Gallaher, T. N.; Schreiner, S. *Organometallics* **1995**, *14*, 1070−1072.

(6) (a) Ciriano, M.; Green, M.; Howard, J. A. K.; Murray, M.; Spencer, J. L.; Stone, F. G. A.; Tsipis, C. A. In *Transition Metal Hydrides*; Bau, R., Ed.; Advances in Chemistry 167; American Chemical Society: Washington, DC, 1978; pp 111−121. (b) Auburn, M.; Ciriano, M.; Howard, J. A. K.; Murray, M.; Pugh, N. J.; Spencer, J. L.; Stone, F. G. A.; Woodward, P. *J. Chem. Soc., Dalton Trans.* **1980**, 659−666.

(7) Heyn, R. H.; Tilley, T. D. *J. Am. Chem. Soc.* **1992**, *114*, 1917−1919.

(8) Shimada, S.; Tanaka, M.; Honda K. *J. Am. Chem. Soc.* **1995**, *117*, 8289−8290.

(9) Michalczyk, M. J.; Recatto, C. A.; Calabrese, J. C.; Fink, M. J. *J. Am. Chem. Soc.* **1992**, *114*, 7955−7957.

(10) Levchinsky, Y.; Rath, N.; Braddock-Wilking, J. *Organometallics* **1999**, *18*, 2583−2585.

(11) (a) Zarate, E. A.; Tessier-Youngs, C. A.; Youngs, W. J. *J. Am. Chem. Soc.* **1988**, *107*, 4068−4070. (b) Zarate, E. A.; Tessier-Youngs, C. A.; Youngs, W. J. *J. Chem. Soc., Chem. Commun.* **1989**, 577−578. (c) Anderson, A, B.; Shiller, P.; Zarate, E. A.; Tessier-Youngs, C. A.; Youngs, W. J. *Organometallics* **1989**, *8*, 2320−2322. (d) Kennedy, V. O.; Zarate, E. A.; Tessier-Youngs, C. A. In *Inorganic and Organometallic Oligomers and Polymers: Proceedings of the 33rd IUPAC Symposium on Macromolecules*; Harrod, J. F., Laine, L. M., Eds.; Kluwer Academic: Boston, MA, 1991; pp 13−22.

(12) Anderson, A, B.; Shiller, P.; Zarate, E. A.; Tessier-Youngs, C. A.; Youngs, W. J. *Organometallics* **1989**, *8*, 2320−2322.

(13) (a) Liu X.; Palacios A. A.; Novoa J. J.; Alvarez, S. *Inorg. Chem.* **1998**, *37*, 1202−1212. (b) Alvarez, S.; Alemany, P.; Aullón, G.; Palacios, A. A.; Novoa J. J. In *The Synergy Between Dynamics and Reactivity at Clusters and Surfaces*; Farrugia, L. J., Ed.; Kluwer Academic: Dordrecht, 1995; pp 241−255. (c) Aullón, G.; Alemany, P.; Alvarez, S. *J. Organomet. Chem.* **1994**, *478*, 75−82. (d) Alemany, P.; Alvarez, S. *Inorg. Chem.* **1992**, *31*, 4266−4275.

(14) Kim, Y.-J.; Lee, S.-C.; Park, J.-I.; Osakuda, K.; Choi, J.-C.; Yamamoto, T. *Organometallics* **1998**, *17*, 4929−4931.

10.1021/om9908711 CCC: $19.00
Publication on Web 12/23/1999

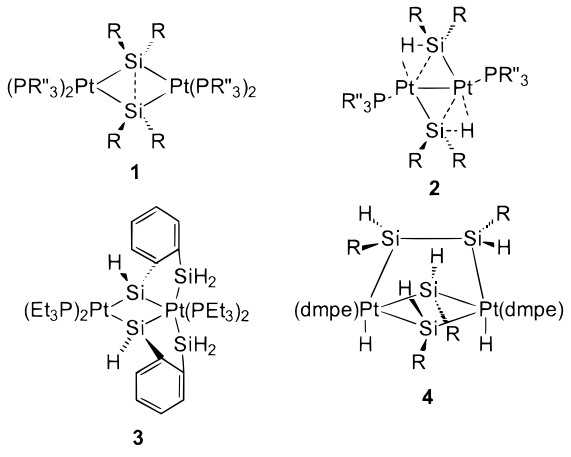

Å).[8,15,16] However, ring **3** differs from **1** in that the two platinum atoms are of different formal oxidation states. Ring **4** is an example of a $(Pt-Si)_2$ ring that shows no short cross-ring distances.[7] Ring **4** shows a Si−Si cross-ring distance considerably larger than known Si−Si bonds (2.882(6) Å), less acute Pt−Si−Pt angles (74° and 75°), and a large Pt−Pt separation (3.7987 Å).[7] Compounds **1**−**4** show that the complete range of cross-ring distances is possible in $(Pt-Si)_2$ rings.

The structure, bonding, and reactivity of four-membered $(M-E)_2$ rings (M = transition metal, E = main-group element) are topics of current interest.[3,13,17] Especially of interest is the interconversion of various structural types of $(M-E)_2$ rings. Certain $(Cu-O)_2$ rings, which are models for oxyhemocyanin, possess O−O or Cu−Cu cross-ring bonds depending on the nature of the ligands on the copper atom.[13,18] An alternative way to change the structure of a $(M-E)_2$ ring is through a redox process. In $(Pt-E)_2$ (E = P or S) rings, the formation of cross-ring Pt−Pt or E−E bonds has been induced by oxidation.[19] Interconversions among the rings **1**−**4** have been investigated. An interconversion of a ring of structure **2** to **1** has been recently reported,[10] whereas an attempt to convert **1** to **4** failed.[7]

In this paper, we also address the question of whether rings of structures **1** and **2** can be interconverted. Tilley's synthesis of three examples of structure **1** involved the reaction of $Pt(PEt_3)_3$ and primary aryl silanes.[7] The reagents were combined in a 2:1 ratio, not the ratio one would expect to use to make rings of structure **1**. To account for this ratio, the balanced equation for Tilley's synthesis must involve additional platinum products. Herein we report the reactions of $Pt(PR_3)_3$ (R = Et, Pr) with the primary alkyl silane Si(Hex)H_3 (Hex = *n*-hexyl), also in a 2:1 ratio. These reactions give rings of both structures **1** and **2** in varying amounts depending on the reaction conditions. We present evidence that the rings of structure **2** are formed from the reaction of **1** with the platinum byproducts present in the mixture. Rings of structures **1** and **2** were completely characterized by multinuclear 1D- and 2D-NMR spectroscopy and by X-ray crystallography.

Experimental Section

General Procedures and Materials. All manipulations were performed under argon or nitrogen using standard anaerobic techniques.[20] Pentane, hexane, and toluene (Fisher) were treated with H_2SO_4 (Fisher) to remove unsaturated impurities, neutralized with dilute aqueous NaOH (Fisher), washed with deionized water, predried over molecular sieves, and distilled immediately before use from sodium/benzophenone ketyl. Ethanol (200 proof) (Quantum) and deionized water were deoxygenated by bubbling argon through them for at least 15 min. Deuterated NMR solvents (Aldrich) were stored over freshly regenerated 3 Å molecular sieves under argon or nitrogen. Silanes (Gelest) were stored over CaH_2 (Aldrich) under argon or nitrogen. K_2PtCl_4 (Strem), H_2 (Praxair), KOH (Fisher), and phosphines (Aldrich) were used without further purification. $Pt(PEt_3)_3$ was prepared according to the literature procedure.[21] *Caution! PEt_3 and PPr_3 are malodorous, pyrophoric, and harmful if inhaled.* Elemental analyses were performed by E & R Microanalytical Laboratories. General comments about NMR spectra are given in a separate section.

Further Characterization of $H_2Pt(PEt_3)_3$.[22] $Pt(PEt_3)_4$ (0.22 g, 3.3×10^{-4} mol) was placed in an NMR tube equipped with a Teflon vacuum valve (Wilmad). It was converted to $Pt(PEt_3)_3$ in vacuo[21] and deuterated toluene (0.7 mL) was added to the tube. Hydrogen was bubbled over the solution for about 30 min. The tube was *immediately* cooled to −40 °C. NMR spectra of $H_2Pt(PEt_3)_3$ were obtained at −50 °C. ^{1}H NMR (C_7D_8): δ ~0.5−2.0 (overlapping m), −13.14 (t of q, $^1J_{Pt-H}$ = 639 Hz, $^2J_{P-H}$ = 18 Hz). ^{13}C NMR (C_7D_8): δ 25.5 (s), 9.0 (s). ^{31}P NMR (C_7D_8): δ −3.85 (s, $^1J_{Pt-P}$ = 3049 Hz). ^{195}Pt NMR (C_7D_8): δ −5859 (q of t, $^1J_{Pt-P}$ = 3042 Hz, $^1J_{Pt-H}$ = 640 Hz).

Degradation of $H_2Pt(PEt_3)_3$. (a) *Under H_2*: The above NMR sample was allowed to warm to room temperature. ^{1}H NMR (C_7D_8): δ ~0.5−2.0 (overlapping m), ~−10.0 (br, apparent t). ^{31}P NMR (C_7D_8): δ ~2.0 (br). ^{195}Pt NMR (C_7D_8): δ −5300 to −5900 (br, m). (b) *With removal of H_2 and solvent*: A sample of $H_2Pt(PEt_3)_3$ was dissolved in C_6D_6, placed in a valved NMR tube (Wilmad). Argon was bubbled into the tube to remove the H_2 gas, and the tube was allowed to stand at room

(15) Using data provided in ref 13, a cross-ring Si−Si distance of 2.720 Å was calculated for **3**.

(16) (a) Lukevics, E.; Pudova, O.; Strokovich, R. *Molecular Structure of Organosilicon Compounds*; Ellis Horwood: Chichester, UK, 1989; Chapter 3.6.1. (b) Sheldrick, W. S. In *The Chemistry of Organic Silicon Compounds*; Patai, S., Rappoport, Z., Eds.; John Wiley & Sons: New York, 1989; Chapter 3. (c) Kaftory, M.; Kapon, M.; Botoshansky, M. In *The Chemistry of Organic Silicon Compounds*, Vol. 2; Rappoport, Z., Apeloig, Y., Eds.; Part 1, Chapter 5.

(17) Some examples: (a) Fehlner, T. P. In *Inorganometallic Chemistry*; Fehlner, T. P., Ed.; Plenum: New York, 1992; Chapter 2. (b) Whitmire, K. H. *Adv. Organmet. Chem.* **1998**, *42*, 1−145. (c) Mathur, P. *Adv. Organomet. Chem.* **1997**, *41*, 243−314. (d) Lotz, S.; van Rooyen, P. H.; Meyer, R. *Adv. Organomet. Chem.* **1995**, *37*, 219−320. (e) Pindado, G. J.; Thorton-Pett, M.; Bochmann, M. *Chem. Commun.* **1997**, 609−610. (f) Üffing, C.; Ecker, A.; Köppe, R.; Schnöckel, H. *Organometallics* **1998**, *17*, 2373−2375. (g) Garcia, J. J.; Arevalo, A.; Montile, V.; Del Rio, F.; Quiroz, B.; Adams, H.; Maitlis, P. M. *Organometallics* **1997**, *16*, 3216−3220. (h) Jemmis, E. D.; Giju, K. T. *Angew. Chem., Int. Ed. Engl.* **1997**, *36*, 606−608. (i) Klabunde, T.; Krebs, B. *Struct. Bonding* **1997**, *89*, 177−198. (j) Negeshi, E. *Chem. Eur. J.* **1999**, *5*, 411−420. (k) Schäfer, K.-O.; Bittl, R.; Zweygart, W.; Lendzian, F.; Haselhorst, G.; Weymüller, T.; Wiegardt, K.; Lubitz, W. *J. Am. Chem. Soc.* **1998**, *120*, 13104−13120. (l) Siegbahn, P. E. M.; Crabtree, R. H. *J. Am. Chem. Soc.* **1999**, *121*, 117−127. (m) Lee, D.; Lippard, S. J. *J. Am. Chem. Soc.* **1998**, *120*, 12153−12154.

(18) (a) Karlin, K. D.; Kaderli, S.; Zuberbühler, A. D. *Acc. Chem. Res.* **1997**, *30*, 139−147. (b) Tolman, W. B. *Acc. Chem. Res.* **1997**, *30*, 227−237.

(19) (a) Ma, A. L.; Thoden, J. B.; Dahl, L. F. *J. Chem. Soc., Chem. Commun.* **1992**, 1516−1518. (b) Leoni, P.; Pasquali, M.; Fortunelli, A.; Germano, G.; Albanati, A. *J. Am. Chem. Soc.* **1998**, *120*, 9564−9573. (c) Leoni, P.; Chiardonna, G.; Pasquali, M.; Marchetti, F. *Inorg. Chem.* **1999**, *38*, 253−259.

(20) Shriver, D. F.; Drezdzon M. A. *The Manipulation of Air-Sensitive Compounds*, 2nd ed.; Wiley: New York, 1986.

(21) (a) Yoshida, T.; Matsuda, T.; Otsuka, S. *Inorg. Synth.* **1990**, *28*, 119−121. (b) Yoshida, T.; Matsuda, T.; Otsuka, S. *Inorg. Synth.* **1990**, *28*, 121−123.

(22) (a) Gerlach, D. H.; Kane, A. R.; Parshall, G. W.; Jesson, J. P.; Muetterties, E. L. *J. Am. Chem. Soc.* **1971**, *93*, 3543−3544. (b) Paonessa, R. S.; Trogler, W. C. *J. Am. Chem. Soc.* **1982**, *107*, 1138−1140.

temperature for 7 days. The volatile components were removed under vacuum, and 0.7 mL of C_6D_6 was added. The sample was left at room temperature for two more days. ^{1}H NMR (C_6D_6): δ 0.86 (overlapping d of t, CH_3, $^1J_{H-H} = 7.7$ Hz, $^2J_{H-P} = 15.6$ Hz), ~0.95−1.2 (overlapping m), 1.5−1.8 (br m). ^{31}P NMR (C_6D_6): δ −4−22 (several weak multiplets), 42.5 (s with Pt satellites, $^1J_{P-Pt} = 4207$ Hz, $Pt(PEt_3)_3$), 46.3 (s, $OPEt_3$).

Degradation of $Pt(PEt_3)_3$. A sample of $Pt(PEt_3)_3$ was dissolved in pentane and placed in a valved NMR tube (Wilmad). The volatile components were then removed under vacuum, and the bright orange residue was allowed to stand at room temperature for 36 h. ^{1}H NMR (C_6D_6): δ 0.87 (overlapping d of t, CH_3 of $Pt(PEt_3)_3$, $^1J_{H-H} = 5.7$ Hz, $^2J_{H-P} = 10.8$ Hz), ~1.0−1.2 (overlapping m), 1.5−1.8 (br m). ^{31}P NMR (C_6D_6): δ 21.4 (s with Pt satellites, $^1J_{P-Pt} = 3514$ Hz), 42.5 (s with Pt satellites, $^1J_{P-Pt} = 4208$ Hz, $Pt(PEt_3)_3$), 47.0 (s, $OPEt_3$).

Preparation of $Pt(PPr_3)_3$. To a solution of KOH (0.3536 g, 6.36 mmol) dissolved in a mixture of 15 mL of EtOH and 0.5 mL of deionized H_2O was added PPr_3 (2.0 mL, 10 mmol) by syringe. A second solution of $K_2[PtCl_4]$ (0.7542 g, 1.82 mmol), dissolved in 5.00 mL of deionized H_2O, was transferred slowly over a period of at least 30 min via cannula into the first solution. The initial pink solution changed quickly into a colorless liquid with a white precipitate. The mixture was stirred for at least 1 h at room temperature and then heated to 60 °C for 3 h. Removal of volatile components under vacuum produced an orange oil, which was extracted with two 15 mL portions of pentane filtered through a frit. After removal of the volatile components under vacuum, $Pt(PPr_3)_3$ was isolated as an orange oil. The crude product, obtained in nearly quantitative yield, contained $OPPr_3$ as an impurity. All attempts to remove $OPPr_3$ lead to decomposition. ^{1}H NMR (C_6D_6): δ 1.15 (t, 3H, CH_3, $^3J = 7.0$ Hz) 1.55−1.75 (m, 4H, CH_2CH_2). ^{31}P NMR (C_6D_6): δ 32 (s, $^1J_{P-Pt} = 4212$ Hz). ^{195}Pt NMR (C_6D_6): δ −4713 (q, $^1J_{Pt-P} = 4198$ Hz).

Preparation of Mixtures of $[Pt(PEt_3)_2SiH(n\text{-Hexyl})]_2$ (1a) and $[(Et_3P)Pt(\mu\text{-Si}(\mu\text{-H})(n\text{-Hexyl})(Pt(PEt_3)_2)H)]_2$ (2a). (a) *A 3:1* ***1a/2a*** *mixture*: $Pt(PEt_3)_3$ (0.280 g, 0.520 mmol) was dissolved in approximately 5 mL of hexane. The reaction was carried out in an open system by allowing argon to flow through an open bubbler attached to the reaction flask. Si(*n*-Hexyl)H_3 (0.040 mL 0.246 mmol) was added via syringe, and a gas (presumably H_2) was immediately produced. The reaction mixture bubbled vigorously for about 10 s before decreasing in rate. The reaction was allowed to stir for exactly 20 min. The reaction was stopped by cooling the flask to −78 °C and removing volatile components under vacuum after the flask was allowed to warm to room temperature. A brown tarry substance resulted (crude yield: 0.085 g) that contained a 3:1 mixture (by ^{1}H NMR) of **1a** (roughly 2:3 ratio of trans to cis isomers by ^{1}H NMR) and **2a** with $OPEt_3$ and $Pt(PEt_3)_3$ present as impurities. The tar was dissolved in approximately 5 mL of hexane, and over several weeks time, **2a** separated out as large orange-red crystals suitable for X-ray analysis. Data for the mixture of **1a** and **2a**: IR (Nujol mull) 1630 cm^{-1} (br, Pt(1)−H-Si(1) of **2a**), 2006 cm^{-1} (s, Pt(3)−H of **2a**), 1985 cm^{-1} (m, Si(1)−H of **1a**); ^{1}H NMR (C_6D_6) δ ~0.9−2.2 (overlapping m, alkyl H of both **1a** and **2a**), 4.01 (apparent pentet, Si(1)−H ***trans*-1a**, $^2J_{Pt(1)-H} = 28$ Hz, $^3J_{P-H} = 14$ Hz), 3.55 (m, Si(1)−H ***cis*-1a**); −2.23 (d of d, Pt(3)−H of **2a,** $^2J_{P(4)-H} = 150$ Hz, $^2J_{P(3)-H} = 26$ Hz, $^2J_{Pt(3)-H} = 1005$ Hz); ^{31}P NMR (C_6D_6) δ 19.5 (s with complex splitting pattern, ***trans*-1a**), 18.1 (s with complex splitting pattern, ***cis*-1a**), 23.6 (d w/Pt satellites, P(1) of **2a**, $^1J_{P(1)-Pt(1)} = 2467$ Hz, $^4J_{P(1)-P(3)} = 12.9$ Hz) 25.2 (complex m w/Pt satellites, P(4) of **2a**, $^1J_{P(4)-Pt(3)} = 2380$ Hz), 27.2 (t of m, P(3) of **2a**, $^1J_{P(3)-Pt(3)} = 1340$ Hz, $^2J_{P(3)-Pt(1)} = 134$ Hz, $^4J_{P(3)-P(1)} = 5.7$ Hz); ^{29}Si NMR (C_6D_6) δ −66 (t of t, ***cis*-1a**, $^2J_{Si(1)-P(1)} = 110$ Hz, $^2J_{Si(1)-P(2)} = 25$ Hz), $^1J_{Si(1)-Pt(1)} = 676$ Hz) −93 (t of t, ***trans*-1a**, $^2J_{Si(1)-P(1)} = 108$ Hz, $^2J_{Si(1)-P(2)} = 16$ Hz, $^1J_{Si(1)-Pt(1)} = 667$ Hz), 194 (apparent t of m, **2a**, $^1J_{Si(1)-Pt(1)} = 1080$ Hz with unresolved couplings); ^{195}Pt NMR (C_6D_6) δ-4801 (***cis*-1a**, apparent t of t, $^1J_{P(3)-Pt(1)} = 1633$ Hz, $^3J_{P(1)-Pt(1)} = 156$ Hz), −4944 (m, Pt(1) of **2a**), $^1J_{P(1)-P(1)} = 2433$ Hz, $^2J_{P(1)-P(2)} = 1355$ Hz)-5500 to −5650 (Pt(3) of **2a**). (b) *A 9:1* ***1a/2a*** *mixture*: This reaction was conducted with no stirring. $Pt(PEt_3)_3$ (0.255 g, 0.648 mmol) was dissolved in approximately 10 mL of pentane. The solution was cooled to −196 °C, and SiH_3(*n*-Hex) (0.0390 mL, 0.241 mmol) was vacuum distilled into the reaction flask. The solution was warmed to −30 °C (~5−10 min), and then the volatiles were removed in vacuo. The resultant orange solid was recrystallized by adding approximately 1 mL of pentane, cooling to −78 °C, and filtering the crystals. The product proved to be a 9:1 mixture (by ^{1}H NMR) of **1a** (roughly 3:1 cis to trans isomers by ^{1}H NMR) and **2a** by ^{1}H, ^{29}Si, and ^{31}P NMR spectroscopies. Present as impurities were $Pt(PEt_3)_3$ and $OPEt_3$ (~5−10% each as estimated by ^{31}P NMR peak heights).

Preparation of $[Pt(PPr_3)_2SiH(n\text{-Hexyl})]_2$ (1b). (a) *Closed-system reaction*: The reaction of $Pt(PPr_3)_3$ (1.10 g, 1.63 mmol) with Si(*n*-Hex)H_3 (0.132 mL, 0.814 mmol) in approximately 10 mL of pentane was carried out using the same procedure listed above in part a, with note of the following changes. The reaction, carried out in a closed system to contain the gas, was stirred overnight before being cooled to −78 °C and filtered. The resultant yellow powder (0.23 g, 40% based on Pt) proved to be predominately compound ***trans*-1b**, a small amount of ***cis*-1b**, and trace amounts of **2b**. $Pt(PPr_3)_3$ and $OPPr_3$ were present as minor impurities. Spectral data are given below. (b) *Open-system reaction*: The reaction above was carried out using the same basic procedure listed for the mixtures of **1a** and **2a,** part a, with note of the following changes. The solution of $Pt(PPr_3)_3$ (1.20 g, 1.78 mmol) in 20 mL of pentane was cooled to 0 °C, and argon was bubbled into the solution and vented through a septum and a needle. Si(*n*-Hexyl)H_3 (0.144 mL, 0.889 mmol) was added via syringe. After about 1 h, the solution was cooled to −78 °C, and the remaining liquid was decanted off the X-ray quality crystals of **1b** (0.21 g, 40% based on Pt). $Pt(PPr_3)_3$ and $OPPr_3$ were present in small amounts as impurities. Data for **1b**: Anal. Calcd for $Pt_2Si_2P_4C_{48}H_{112}$: C, 45.77; H, 8.96. Found: C, 44.54; H, 8.96. IR (Nujol mull): 1984 cm^{-1} (m, Si(1)−H). ^{1}H NMR (C_6D_6): δ ~0.9−2.1 (overlapping m, alkyl H), 3.89 (apparent septet, Si(1)−H ***trans*-1b**, $^1J_{Si(1)-H} = 159$ Hz, $^2J_{Pt(1)-H} = 26$ Hz, $^3J_{P-H} = 15$ Hz); ~3.54 (br, w, Si−H ***cis*-1b**), integration ***trans*-1b**/***cis*-1b** ≈ 15:1. ^{13}C NMR (C_6D_6): δ 14−21 (m, P−Pr), 32.5 (m, Si-hexyl), 37.8 (apparent t, Si-hexyl). ^{31}P NMR (C_6D_6): δ 15.8 (s with complex splitting,[23] trans isomer) 12.4 (s with complex splitting,[23] cis isomer). ^{29}Si NMR (C_6D_6): δ −94 (t of t, $^2J_{Si(1)-P(1)} = 101$ Hz, $^2J_{Si(1)-P(2)} = 16$ Hz, $^1J_{Si(1)-Pt(1)} = 660$ Hz). ^{195}Pt NMR (C_6D_6): δ −4777 (apparent t of t, $^1J_{Pt(1)-P(3)} = 1740$ Hz, $^1J_{Pt(1)-H} = 29$ Hz).

Preparation of $[(Et_3P)Pt(\mu\text{-Si}(\mu\text{-H})(n\text{-Hexyl})(Pt(PEt_3)_2)H)]_2$ (2a). The reaction of $Pt(PEt_3)_3$ (0.820 g, 1.49 mmol) and Si(*n*-Hexyl)H_3 (0.125 mL, 0.772 mmol) in 10 mL of hexane was carried out in a closed system to contain the gas generated, in a fashion similar to the closed-system reaction of **1b**. The following changes were made. The reaction was stirred for 36 h. Removal of volatile components under vacuum produced a reddish-orange viscous oil with yellow microcrystalline solids. Approximately 5−10 mL of toluene was added to the flask, and the solution was cooled to −78 °C. Filtration produced a yellow powder. The yellow powder was dissolved in approximately 5 mL of toluene, and over several weeks time, large crystals of **2a** formed without cooling or concentration of the solution (0.14 g, 22% yield based on platinum). Data for **2a**: Anal. Calcd for $Pt_4Si_2P_6C_{48}H_{120}$: C, 33.52; H, 7.03. Found: C, 33.89; H, 7.17. IR (Nujol mull): cm^{-1} 1630 cm^{-1} (w, br, Pt(1)−H-Si(1)). ^{1}H NMR: δ −2.23 (d of d with Pt satellites, Pt(3)−H, $^2J_{P(4)-H} = 150.3$ Hz, $^2J_{P(3)-H} = 26.1$ Hz, $^2J_{Pt(3)-H} = 998$ Hz), ~0.9−2.5 (overlapping m, alkyl H). ^{31}P NMR (C_6D_6): δ 23.6 (d w/Pt satellites, P(1) of **2a**, $^1J_{P(1)-Pt(1)} =$

(23) Spectra that illustrate the complex splitting pattern are shown in ref 10.

Table 1. Crystal Data and Structure Refinement for *trans*-1b and 2a

	***trans*-1b**	**2a**
empirical formula	$C_{48}H_{110}P_4Pt_2Si_2$	$C_{48}H_{120}P_6Pt_4Si_2$
fw	1257.60	1719.80
temperature	173(2) K	147 K
wavelength	0.71073 Å	0.71073 Å
cryst syst	triclinic	monoclinic
space group	$P\bar{1}$	$P2(1)/c$
unit cell dimens	$a = 12.739(5)$ Å $b = 19.399(6)$ Å $c = 25.361(10)$ Å $\alpha = 90.44(4)°$ $\beta = 104.35(3)°$ $\gamma = 91.17(3)°$	$a = 26.649(5)$ Å $b = 11.469(3)$ Å $c = 23.587(5)$ Å $\beta = 115.488(14)°$
volume	6070(4) Å^3	6507(2) Å^3
Z	4	4
density (calcd)	1.376 Mg/m^3	1.755 Mg/m^3
abs coeff	4.776 mm^{-1}	8.784 mm^{-1}
$F(000)$	2568	3336
crystal size	0.50 × 0.40 × 0.30 mm^3	0.5 × 0.26 × 0.16 mm^3
θ range for data collection	1.94−22.50°	1.91−22.50°
index ranges	$-13 \le h \le 1$, $-20 \le k \le 20$, $-26 \le l \le 27$	$-28 \le h \le 25$, $0 \le k \le 12$, $0 \le l \le 25$
no. of reflns collected	17 795	13 387
no. of ind reflns	15393 ($R_{int} = 0.0513$)	11252 ($R_{int} = 0.0442$)
ab corr	96.9% ψ-scan	semiempirical from ψ-scans, XABS2[30]
max. and min. transmission	0.3284 and 0.1987	1.0000 and 0.3188 (from ψ-scans)
refinement method	full-matrix least-squares on F^2	full-matrix least-squares on F^2
no. of data/restraints/params	15393/36/529	8424/2/365
goodness-of-fit on F^2	1.032	1.040
final R indices [$I > 2\sigma(I)$]	R1 = 0.0896, wR2 = 0.1774	R1 = 0.0394, wR2 = 0.0666
R indices (all data)	R1 = 0.1604, wR2 = 0.2000	R1 = 0.0760, wR2 = 0.0694
largest diff. peak and hole	2.709 and −1.600 e Å^{-3}	1.790 and −1.217 e Å^{-3}

2467 Hz, $^4J_{P(1)-P(3)} = 12.9$ Hz), 25.2 (complex m w/Pt satellites, P(4) of **2a**, $^1J_{P(4)-Pt(3)} = 2380$ Hz), 27.2 (t of m, P(3) of **2a**, $^1J_{P(3)-Pt(3)} = 1340$ Hz, $^2J_{P(3)-Pt(1)} = 134$ Hz, $^4J_{P(3)-P(1)} = 5.7$ Hz). ^{29}Si NMR (C_6D_6) δ 194 (apparent t of m), ($J_{Si(1)-Pt(1)} = 1080$ Hz and unresolved couplings). ^{195}Pt NMR (C_6D_6): δ −4944 (complex m, Pt(1)), −5500 to −5650 (2 broad multiplets, Pt(3)).

Reaction of 1a with H_2 and $Pt(PEt_3)_4$. In a flask, $Pt(PEt_3)_4$ (0.80 g, 0.073 mmol) was dissolved in 5 mL of pentane, and H_2 was bubbled into the solution at room temperature. In a second flask, **1a** (0.80 g, 0.073 mmol) was dissolved in 5 mL of pentane and transferred, via cannula, into the flask containing the $Pt(PEt_3)_4$. The H_2 bubbling was maintained for approximately 5 min after transfer was complete. After allowing the reaction to stir overnight, the volatile components were removed under vacuum, and a brown residue containing **2a** resulted. The spectroscopic data were identical to that obtained for crystalline **2a**.

X-ray Crystallography. Crystal data, data collection and reduction, and structure refinement details for $C_{48}H_{110}P_4Pt_2Si_2$ (**1b**) and $C_{48}H_{120}P_6Pt_4Si_2$ (**2a**) are listed in Table 1.

Crystal Data and Structure Refinement for 1b. Intensity data were collected at low temperature, 173 K, on a Syntex $P2_1$ diffractometer using Mo Kα radiation ($\lambda = 0.71073$ Å). Unit cell dimensions were determined from 12 centered reflections and refined using 30 centered reflections, $20.0° \le 2\theta \le 30.0°$. The structure of **1b** was solved using a combination of direct methods and difference Fourier syntheses, SHELXTL,[24] and refined using full-matrix least-squares (SHELXL-93).[25]

A semiempirical absorption correction was applied using ψ-scan data to yield minimum and maximum transmission coefficients of 0.19870 and 0.3284. During refinement it proved necessary to restrain the *n*-hexyl groups and certain *n*-propyl groups so as to give chemically acceptable distances and angles. In general the 1,2 distances were restrained to 1.54(2) Å, while the 1,3 distances were restrained to 2.50(4) Å. Data greater than 45° were omitted from the final refinement as were data less than $0.5\sigma(F^2_o)$. Platinum, silicon, and phosphorus atoms of **1b** were refined using anisotropic thermal parameters, but all carbon atoms were refined isotropically due to the restraints applied to the model. All hydrogen atoms were placed in calculated positions and refined using a riding model. Refinement of 529 parameters on 15 393 data with 36 restraints produced *R*-indices R1[26] = 8.96% for $F^2 > 2\sigma(F^2)$ and wR2[27] of 20.00% with a goodness of fit of 1.032.[28]

Crystal Data and Structure Refinement for 2a. Intensity data were collected at low temperature, 147 K, on a Syntex $P2_1$ diffractometer using Mo Kα radiation ($\lambda = 0.71073$ Å). Unit cell dimensions were determined from 13 centered reflections, $4.98° \le 2\theta \le 20.19°$ and refined using 24 centered reflections, $15.35° \le 2\theta \le 28.70°$. The structure was solved using a combination of direct methods (SIR92[29]) and difference Fourier syntheses (SHELXTL[24]) and refined using full-matrix least-squares (SHELXL-93[25]).

The data for **2a** showed an average 51% decrease in transmitted intensity during azimuthal scans and a linear absorption coefficient of 8.784 mm^{-1}. A semiempirical absorption correction was applied using ψ-scan data to yield minimum and maximum transmission coefficients of 0.3188 and 1.0000. Refinement of the *n*-hexyl and ethyl groups, however, without the use of distance restraints produced chemically unacceptable distances and angles. Further attempts to refine

(24) Sheldrick, G. M. *SHELXTL Version 5.1. Structure Determination Software Programs*; Bruker Analytical X-ray Systems, Inc.: Madison, WI, 1997.

(25) Sheldrick, G. M. *SHELXL-93 Program for the refinement of crystal structures*; Univ of Göttingen: Germany, 1993.

(26) $R1 = \sum||F_o| - |F_c||/\sum|F_o|$. Conventional *R*-factors are calculated using the observed criterion. This criterion is irrelevant to the choice of reflections used in the refinement.

(27) $wR2 = [\sum[w(F_o^2 - F_c^2)^2]/\sum[w(F_o^2)^2]]^{1/2}$. Weighted *R*-factors are based on F^2 and are statistically about twice as large as those based on *F*.

(28) $S = [\sum[w(F_o^2 - F_c^2)^2]/(n - p)]^{1/2}$, where $w = 1/[\sigma^2(F_o^2) + (0.0127P)^2]$, where $P = (F_o^2 + 2F_c^2)/3$. The goodness of fit is based on F^2, where n = number of data and p = number of parameters refined.

(29) Altomare, A.; Burla, M. C.; Camalli, M.; Cascarano, G.; Giacovazzo, C.; Guagliardi, A.; Polidori, G. *J. Appl. Crystallogr.* **1994**, *27*, 435−436.

anisotropic displacement parameters for any of the carbon atoms yielded meaningless results. A further Fourier absorption correction, XABS2,[30] was thus applied to the isotropic model previously refined using the ψ-scan corrected data. Such data provided a much better starting set for the calculation of structure factors for use in the program XABS2 than the uncorrected data set. Because the nature of this crystal structure is that of a few strongly absorbing atoms surrounded by many lighter atoms, the diffraction pattern is dominated by the heaviest atoms. This implies that the overall scale factor and the thermal factors of the platinum atoms are strongly correlated such that the thermal factors for lighter atoms cannot be refined satisfactorily. Hence the thermal parameters of the platinum atoms were held fixed at a reasonable value, U(eq) of 20 Å^2 × 10^3, prior to application of XABS2 so as to account for the gross effects of absorption. Further restraints were applied to the isotropic model prior to the correction so as to ensure as much validity to the calculated structure factors as possible: the 1,2 distances of the *n*-hexyl groups were restrained to 1.54(1) Å, the 1,2 distances of the ethyl groups were restrained to a common free variable that refined to 1.56(1) Å, the phosphorus−carbon distances were restrained to a common free variable that refined to 1.83(1) Å, and the thermal factors of the ethyl group carbons were restrained to common free variables that refined to U(eq) values of 39.9(1.9) and 54(2) Å^2 × 10^3 for methylene and methyl carbons, respectively. Data with intensities less than the observed criterion, $2\sigma I$, were omitted prior to the correction, as were data greater than 45° in 2θ. After the correction all restraints were eventually removed from the model, and only data greater than 45° in 2θ were excluded from the final refinement.

Except for the ethyl group carbon atoms, the non-hydrogen atoms of **2a** were refined using anisotropic thermal displacement parameters. Hydrogen atoms were placed in calculated positions and refined using a riding model. The two terminal platinum hydrides and the two agostic hydrides could not be refined with certainty from the difference Fourier maps and, hence, were omitted from the model. Carbon atom C26 was judged to be disordered over two sites with occupancies of 66% and 34%. The disordered ethyl group was refined using distance restraints and a common thermal parameter. Refinement of 365 parameters on 8424 data with two restraints produced *R*-indices R1[26] = 3.94% for $F^2 > 2\sigma(F^2)$ and wR2[27] = 6.94% with a goodness of fit[28] of 1.040.

NMR Measurements. The routine ^{1}H, ^{31}P, and ^{29}Si NMR reported in the Experimental Section were obtained on a 300 MHz instrument, using a DEPT pulse sequence for ^{29}Si spectra.[31] 1D ^{195}Pt NMR spectra were collected at room temperature on a Varian VXRS 300 MHz NMR spectrometer. 1D ^{1}H NMR and 2D gradient HMQC[32] experiments were done at 30 ± 0.1 °C on a Varian Unity*plus* 600 MHz NMR spectrometer equipped with a Nalorac 5 mm ^{1}H/^{2}H/^{13}C/X (where X is tunable over the range of the resonance frequencies from ^{15}N to ^{31}P) pulse field gradient probe. C_6D_6 was used as the solvent as well as the internal reference for ^{1}H (δ_H = 7.16 ppm) and ^{13}C (δ_C = 128.39 ppm) chemical shifts. ^{31}P NMR spectra were proton decoupled and referenced externally to 85% H_3PO_4. Tetramethylsilane (TMS) was used as an external reference for ^{29}Si chemical shifts. A 0.1 M $Na_2[PtCl_6]$ solution in H_2O/D_2O (4:1, v/v) was used as an external reference for ^{195}Pt chemical shifts,[33] where $\Xi(^{195}Pt) = 64.$ 500 MHz (300 MHz instrument) or δ = 0 ppm. To test the effect of solvent, the chemical shift of a capillary tube containing 0.1 M $Na_2[PtCl_6]$ in H_2O/D_2O (4:1, v/v) solution in a tube of C_6D_6 was obtained. The resultant shift observed was less than 3 ppm and is considered negligible.

1D-NMR. The ^{1}H spectra of both **1b** and **2a** were acquired at 600 MHz using a 3.0 s acquisition time without ^{31}P decoupling, and 0.5 s acquisition time with ^{31}P (MPF) decoupling, 3.3 μs (30°) pulse width, and 16 transients. The ^{195}Pt spectrum of **1b** was acquired at 64.150 MHz, and the spectrum of **2a** was at 64.148 MHz using 0.1 s acquisition time, 5 μs pulse width, 0.1 s delay, and 204 800 transients. Both were weighted with 50 Hz line broadening before Fourier transformation.

^{1}H−^{195}Pt Long-Range Gradient HMQC 2D-NMR of 1b. This spectrum was collected with ^{1}H and ^{195}Pt 90° pulses of 10.3 and 14.0 μs respectively, a relaxation delay of 1 s, $\Delta = (2 \times {}^2J_{HPt})^{-1} = 17.8$ ms (optimized for 2 bond ^{1}H−^{195}Pt correlations), 4000 and 23571.0 Hz spectral windows in the ^{1}H(*f2*) and ^{195}Pt(*f1*) chemical shift dimensions, respectively, and a 0.256 s acquisition time; eight transients were averaged for each of 1024 real t_1 increments. The gradient strengths of three 2.0 ms pulse field gradients (PFGs) were 0.182, 0.182, and −0.0778 T m^{-1}, respectively. The data were processed with sinebell weighting; the spectrum was displayed in the magnitude-mode in both dimensions; zero filling was used so that 2D FT was performed on an 8192 × 8192 matrix.

^{1}H−^{29}Si Gradient HMQC 2D-NMR Both with and without ^{29}Si (MPF) Decoupling of 1b. These spectra were collected with ^{1}H and ^{29}Si 90° pulses of 10.3 and 14.0 μs, respectively, a relaxation delay of 1 s, $\Delta = (2 \times {}^1J_{HSi})^{-1} = 3.12$ ms (optimized for 1 bond ^{1}H−^{29}Si correlations), 1600 and 21074.8 Hz spectral windows in the ^{1}H(*f2*) and ^{29}Si(*f1*) dimensions, and a 0.260 s acquisition time for the spectrum without ^{29}Si decoupling and 0.048 s acquisition time for the spectrum with ^{29}Si decoupling; 16 transients were averaged for each of 1024 real t_1 increments. The gradient strengths of three 2.0 ms PFGs were 0.182, 0.182, and −0.0723 T m^{-1}, respectively. The data were processed with sinebell weighting; spectra were displayed in the magnitude-mode in both dimensions; 2D FT was performed on an 8192 × 8192 matrix.

2D-NMR of 2a. ^{1}H−^{195}Pt Long-Range Gradient HMQC 2D-NMR of 2a. The spectrum was collected with ^{1}H and ^{195}Pt 90° pulses of 10.6 and 14.0 μs, respectively, a relaxation delay of 1 s, $\Delta = (2 \times {}^nJ_{HPt})^{-1} = 33.3$ ms (optimized for multiple bond ^{1}H−^{195}Pt correlations), a 0.124 s acquisition time, and 4000 and 100 000 Hz spectral windows in the ^{1}H(*f2*) and ^{195}Pt(*f1*) dimensions, respectively; 16 transients were averaged for each of 512 real t_1 increments. The gradient strengths of three 2.0 ms PFGs were 0.182, 0.182, and −0.0778 T m^{-1}, respectively. The data were processed with sinebell weighting; the spectrum was displayed in the magnitude-mode in both dimensions; the data was zero filled so that 2D FT was performed on an 8192 × 8192 matrix.

^{1}H−^{29}Si Gradient HMQC 2D-NMR Both with and without ^{29}Si (MPF) Decoupling of 2a. These spectra were collected with ^{1}H and ^{29}Si 90° pulses of 10.1 and 13.0 μs, respectively, a relaxation delay of 1 s, $\Delta = (2 \times {}^1J_{HSi})^{-1} = 6.67$ ms (optimized for agostic bonding ^{1}H−^{29}Si correlation), 1000 and 26365.8 Hz spectral windows in the ^{1}H(*f2*) and ^{29}Si(*f1*) dimensions, and a 0.128 s acquisition time for the spectrum without ^{29}Si decoupling and 0.048 s acquisition time for the spectrum with ^{29}Si decoupling; eight transients were averaged for each of 512 real t_1 increments. The gradient strengths of three 2.0 ms PFGs were 0.182, 0.182, and −0.0723 T m^{-1}, respectively. The data were processed with sinebell weighting; spectra were displayed in the magnitude-mode in both dimensions; zero filling was used so that 2D FT was performed on an 8192 × 8192 matrix.

Results and Discussion

Synthesis. The reagent $Pt(PPr_3)_3$ was prepared by a similar route used to prepare $Pt(PEt_3)_3$.[21] $Pt(PPr_3)_3$ was

(30) Parkin, S.; Moezzi, B.; Hope, H. *J. Appl. Crystallogr.* **1995**, *28*, 53−56.
(31) Blinka, T. A.; Helmer, B. J.; West, R. *Adv. Organomet. Chem.* **1984**, *23*, 193−218.
(32) Vuister, G. W.; Boelens, R.; Hurd, R. E.; Zijl, P. C. M. *J. Am. Chem. Soc.* **1991**, *113*, 9688−9690.
(33) (a) Freeman, W.; Pregosin, S. N.; Sze, S, N.; Venanzi, L. M. *J. Magn. Reson.* **1976**, *22*, 473−478. (b) Pesek, J. J.; Mason, R. W. *J. Magn. Reson.* **1977**, *25*, 519−529.

obtained as an orange oil directly by the reduction of an aqueous solution of $K_2[PtCl_4]$ with ethanolic KOH in the presence of PPr_3. In contrast to the synthesis of $Pt(PEt_3)_3$, it was not necessary to isolate the tetraphosphine complex as a precursor. The initially colorless solution, consistent with the presence of $Pt(PPr_3)_4$, becomes orange simply by removal of the volatile components under vacuum at room temperature. Prolonged evacuation and/or mild heating is required to convert $Pt(PEt_3)_4$ to $Pt(PEt_3)_3$.[21] Even when using freshly distilled PPr_3, we were unable to prepare $Pt(PPr_3)_3$ without the presence of $OPPr_3$ impurity. The formation of phosphine oxides byproducts in the synthesis of related palladium(0) phosphine complexes from palladium(II) reagents has been reported.[34] As $Pt(PPr_3)_3$ is thermally unstable, several attempts to purify it resulted in rapid decomposition to a black tar, which still contains significant quantities of $Pt(PPr_3)_3$. The black tar interferes with further reactions. Therefore, it is advisable to use $Pt(PPr_3)_3$ within 24 h of its preparation or to store it at −40 °C. $Pt(PPr_3)_3$ was characterized by ^{31}P NMR and ^{195}Pt NMR spectroscopy. The $^{195}Pt-^{31}P$ coupling for $Pt(PPr_3)_3$ of 4210 Hz can be compared to that of $Pt(PEt_3)_3$ at 4220 Hz.[21]

The reaction of $Si(Hex)H_3$ with 2 molar equiv of the platinum(0) complex $Pt(PEt_3)_3$ in hexane produced a mixture of **1a** and **2a** in differing ratios, with the ratio dependent upon the reaction time and amount of dihydrogen present (eq 1). To favor the formation of

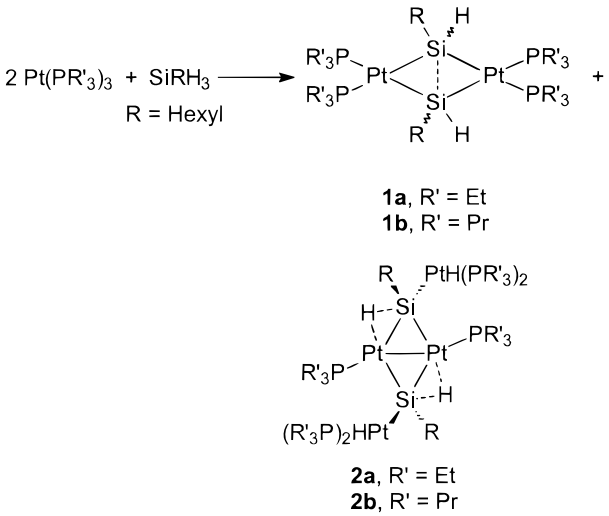

more **1a**, a fast reaction time (∼5 min) at −30 °C and immediate removal of the volatile components (∼5−10 min), especially hydrogen gas, were required. Under such conditions the ratio of **1a** to **2a** was 9:1. If the reaction is allowed to proceed at room temperature for 20 min, a mixture of both **1a** and **2a** in approximately a 3:1 ratio was obtained. If this second reaction is carried out in a closed system for 20 min, a mixture of **1a** and **2a** is obtained (roughly 1:1 by ^1H NMR). Allowing the reaction time to increase to 36 h decreases the amount of **1a** to the point that it is undetectable by ^1H and ^{29}Si and just barely detectable by ^{31}P NMR spectrocopies. Changing the phosphine ligand from PEt_3 to PPr_3 affected the ratio of **1** to **2** as well. The reaction

Scheme 1

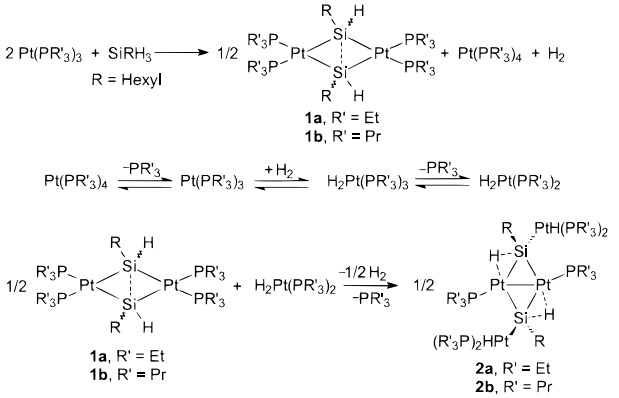

of $Pt(PPr_3)_3$ with $Si(Hex)H_3$ in a 2:1 molar ratio in pentane for ∼15 h afforded predominately **1b**. Trace amounts of **2b** were only detectable by ^{195}Pt NMR spectroscopy on a 600 MHz instrument (see below). Compound **2b** appeared to be a minor product whether the reaction was carried out in an open (argon bubbling) or closed system. The differences between the PEt_3 and PPr_3 cases are difficult to rationalize because the steric and electronic properties of the two phosphines are similar.[35]

Compounds **1a** and **1b** are obtained as mixtures of cis and trans isomers.[36] The cis isomer predominates early in the reaction and is slowly converted to an equilibrium mixture with the trans isomer as the predominant species. Allowing NMR solutions to stand results in the conversion of the cis isomer to the trans. For this reason, the ratios of cis to trans given in the experimental should not be taken very seriously. These observations are consistent with those on similar systems.[11] A study of how different substituents on the silane and the phosphine affect the cis/trans isomerization of **1** is in progress.

Complexes **1a**, **1b**, **2a**, and **2b** are mildly air-sensitive solids that are soluble in aliphatic, aromatic, and etheral solvents. The solutions are highly air-sensitive and degrade on standing even in evacuated and sealed systems.

An attempt to account for the products in eq 1 is shown in Scheme 1. Tilley and co-workers reported that the reaction of $Pt(PEt_3)_3$ with primary aryl silanes $Si(Ar)H_3$ (Ar = Ph, p-Tol, Mes) in a 2:1 ratio produced compounds of structure **1** in near quantitative yield based on the silane.[7] When the yield is calculated on the basis of the platinum reagent, it is clear that more than half the platinum is lost in this reaction. In eq 1, except for the use of the primary alkyl silane Si(*n*-Hexyl)H_3 rather than primary aryl silanes, reaction conditions similar to those of Tilley were used. The first step in the reaction sequence involves the synthesis of **1**. A possible mechanism for the formation of **1** from zerovalent platinum reagents and silanes has been proposed.[7,9] On a simplistic level, the balanced equation for the synthesis of **1a** from $Pt(PEt_3)_3$ and $Si(Hexyl)H_3$ would require H_2 and $Pt(PEt_3)_4$ to be present as byprod-

(34) McLaughlin, P. A.; Verkade, J. G. *Organometallics* **1998**, *17*, 5937−5940.

(35) (a) Brown, T. L.; Lee, K. J. *Coord. Chem. Rev.* **1993**, *128*, 89−116. (b) Rahman, M. M.; Liu, H.-Y.; Prock, A.; Giering, W. P. *Organometallics* **1989**, *8*, 1−7.

(36) The cis and trans isomers are defined by the confirmation of the silicon substituents relative to the Si−Si vector.

ucts, as shown by the top equation of Scheme 1. However, $Pt(PEt_3)_4$ is known to dissociate PEt_3 to give $Pt(PEt_3)_3$, a species that readily adds hydrogen to give the dihydride $H_2Pt(PEt_3)_3$. Another species that would be present is $H_2Pt(PEt_3)_2$ because $H_2Pt(PEt_3)_3$ is known to dissociate PEt_3.[22] The observation that **1a** is formed early in the reaction but later disappears suggests that **1a** is a precursor to **2a**. The observations that a closed system favors **2a** and that bubbling argon through the reaction mixture or removing the volatiles in vacuo limits the formation of **2a** suggest that H_2 is required for the production of **2a**. To account for the exocyclic $HPt(PEt_3)_2$ moiety of **2a**, reaction of **1a** with $H_2Pt(PEt_3)_2$ or $H_2Pt(PEt_3)_3$ is proposed. Both of these species would require H_2 gas to be formed. Concomitant loss of PEt_3 and H_2 gas would be required to convert a mixture of **1a** and $H_2Pt(PEt_3)_n$ ($n = 2$ or 3) to **2a**. We would expect that the small amount of **2b** observed is formed by an analogous path to **2a**, and therefore, Scheme 1 has been generalized to include **1b** and **2b**.

To test Scheme 1, $H_2Pt(PEt_3)_3$, prepared from H_2 and $Pt(PEt_3)_3$,[22] was reacted with **1a** under conditions in which hydrogen gas was allowed to escape. By ^1H, ^{29}Si, and ^{31}P NMR spectroscopy the major product was **2a**. Also in support of Scheme 1, Braddock-Wilking has observed the opposite interconversion, loss of hydrogen and phosphine from **2** to give **1**. However, the ring of structure **2** did not contain exocyclic platinum substituents.[10] Though conversions of metal-silicon rings with no metal−metal bonds to rings with metal−metal bonds have been observed in a number of systems, the use of a transition-metal hydride to cause such rearrangements appears to be unprecedented.[3] The mechanism by which the platinum-hydride adds to **1a** is under investigation.

In the ^{31}P and ^{195}Pt NMR spectra (see below) of even purified samples of the products from eq 1, several additional resonances due to impurities were often observed. We and others[22] had observed that solutions of $H_2Pt(PEt_3)_3$ and $Pt(PEt_3)_3$ degrade on standing, and therefore, it was suspected that the additional resonances were due to the degradation products. After studying the degradation of $H_2Pt(PEt_3)_3$ and $Pt(PEt_3)_3$, under conditions that are similar to those used to conduct eq 1, these suspicions have been verified. During this study the ^{195}Pt NMR spectrum of $H_2Pt(PEt_3)_3$ at −50 °C was also obtained. It shows a quartet of triplets due to coupling to two hydrides and to the three PEt_3 ligands.

X-ray Crystallography. The crystal structure of the trans isomer of compound **1b** is shown in Figure 1, and selected metrical data that focuses on the four-membered-ring are given in Table 2.

The crystal of ***trans*-1b** contained two slightly different molecules within the asymmetric unit. The substituents on the silicon of ***trans*-1b** lie above and below the four-membered ring, with the two hexyl substituents on opposite sides of the ring in a trans conformation relative to the Si−Si vector. Though only the ***trans*-1b** was observed in the solid state, both trans and cis isomers are observed in solution (see below).

Except for the Pt−Pt nonbonding distances (3.984(2) and 4.005(2) Å), the distances and angles for the two molecules of ***trans*-1b** are within experimental error.

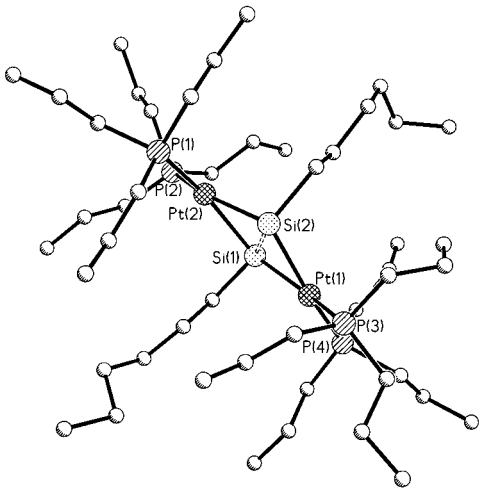

Figure 1. Isotropic plot of the crystal structure of **1b**. Hydrogen atoms are omitted for clarity.

The four-membered rings of ***trans*-1b** are both slightly bent with dihedral angles between the two $PtSi_2$ planes of 169.2(4)° and 169.4(3)°. The small difference in dihedral angles is responsible for the difference in the Pt−Pt nonbonding distances. Two phosphorus atoms are also within each respective $PtSi_2$ plane. The slightly bent structure of ***trans*-1b** is a hybrid between two structures for **1** that we have reported before. Previously, planar rings with trans substituents and a more strongly bent ring (dihedral angle = 132.3°) with cis substituents were characterized.[11] Like the other rings **1**, the Si−Si distances of ***trans*-1b** are within the range of known Si−Si single bonds, which is 2.30−2.70 Å (Si−Si = 2.58−2.60 Å for trans planar **1** and 2.65 Å for the cis bent **1**).[11,16] Other metrical data are also similar to what has been observed in other examples of **1** of formula $[Pt(PEt_3)_2(SiXR')]_2$. Such rings show acute Si−Pt−Si angles (64−67° for both trans and cis), obtuse Pt−Si−Pt angles (trans = 114−116°, cis = 99°), and nonbonded Pt−Pt distances (trans = 3.97−4.05 Å, cis = 3.66 Å).[11]

The crystal structure of compound **2a** is shown in Figure 2, selected metrical data for the four-membered ring of **2a** are given in Table 2, and data for the exocyclic platinum moieties of **2a** are given in Table 3.

In **2a**, Pt(1), Pt(2), Si(1), and Si(2) define a plane with the P(1) and P(2) atoms lying slightly above and below the plane at 0.67(1)° and 2.46(1)°, respectively. The silicon substituents for **2a** lie above and below the plane of the four-membered ring with the two hexyl substituents on opposite sides of the ring in a trans configuration. Both in solution (see below) and in the solid state only the trans configuration is detected. The Si−Si distance of **2a** is clearly nonbonding (3.966(4) Å). The Si−Pt−Si angles (113−114°) are obtuse, and the Pt−Si−Pt angles (66−67°) are acute. The platinum−silicon bond lengths of **2a** alternate around the ring, are in the range 2.347(3)−2.441(4) Å, and are normal.[1a] The average platinum−silicon distance within the $(Pt-Si)_2$ ring (2.393 Å) is slightly greater than the average platinum−silicon distance to the exocyclic $PtH(PEt_3)_2$ moiety (2.376 Å). The alternation of the platinum−silicon bonds of **2a** is consistent with the presence of two agostic hydrides which would bridge the longer platinum−silicon bonds. Large angles at Pt(1) and Pt(2) between the phosphorus

Table 2. Selected Bond Lengths (Å) and Angles (deg) for the Platinum−Silicon Four-Membered Rings of *trans*-1b and 2a

	bonds/angles	***trans*-1b**, molecule A	bonds/angles	***trans*-1b**, molecule B	bonds/angles	2a
Si−Si	Si(1)−Si(2)	2.612(8)	Si(3)−Si(4)	2.598(8)	Si(1)···Si(2)	3.966(4)
Pt−Pt	Pt(1)···Pt(2)	3.984(2)	Pt(3)···Pt(4)	4.005(2)	Pt(1)−Pt(2)	2.6803(8)
Pt−Si	Pt(1)−Si(1)	2.381(6)	Pt(3)−Si(3)	2.390(7)	Pt(1)−Si(1)	2.431(4)
	Pt(1)−Si(2)	2.374(6)	Pt(3)−Si(4)	2.396(6)	Pt(1)−Si(2)	2.347(3)
	Pt(2)−Si(1)	2.408(6)	Pt(4)−Si(3)	2.403(7)	Pt(2)−Si(1)	2.353(3)
	Pt(2)−Si(2)	2.394(7)	Pt(4)−Si(4)	2.387(6)	Pt(2)−Si(2)	2.441(4)
Pt−P	Pt(1)−P(3)	2.313(6)	Pt(3)−P(6)	2.313(6)	Pt(1)−P(1)	2.216(4)
	Pt(1)−P(4)	2.333(6)	Pt(3)−P(5)	2.321(5)	Pt(2)−P(2)	2.212(4)
	Pt(2)−P(1)	2.319(5)	Pt(4)−P(7)	2.319(6)		
	Pt(1)−P(2)	2.319(6)	Pt(4)−P(8)	2.323(6)		
inter-ring angles	Pt(1)−Si(1)−Pt(2)	112.6(2)	Pt(3)−Si(3)−Pt(4)	113.3(3)	Pt(1)−Si(1)−Pt(2)	68.13(9)
	Pt(1)−Si(2)−Pt(2)	113.3(3)	Pt(3)−Si(4)−Pt(4)	113.7(3)	Pt(1)−Si(2)−Pt(2)	68.05(9)
	Si(1)−Pt(1)−Si(2)	66.6(2)	Si(3)−Pt(4)−Si(4)	65.7(2)	Si(1)−Pt(1)−Si(2)	112.18(13)
	Si(1)−Pt(2)−Si(2)	65.9(2)	Si(4)−Pt(3)−Si(3)	65.7(2)	Si(1)−Pt(2)−Si(2)	111.64(13)
extra-ring angle around Si	C(37)−Si(1)−Pt(2)	104.7(10)	C(85)−Si(3)−Pt(3)	105.8(9)	Pt(3)−Si(2)−Pt(2)	127.8(2)
	C(43)−Si(2)−Pt(2)	104.2(8)	C(91)−Si(4)−Pt(3)	106.3(9)	Pt(4)−Si(1)−Pt(1)	128.1(2)
	C(37)−Si(1)−Pt(1)	109.8(10)	C(85)−Si(3)−Pt(4)	109.3(9)	Pt(2)−Si(1)−Pt(4)	113.8(2)
	C(43)−Si(2)−Pt(1)	110.4(8)	C(91)−Si(4)−Pt(4)	107.3(9)	Pt(1)−Si(2)−Pt(3)	117.7(2)
	C(37)−Si(1)−Si(2)	130.4(8)	C(85)−Si(3)−Si(4)	131.4(8)	C(1)−Si(1)−Pt(4)	109.1(4)
	C(43)−Si(2)−Si(1)	114.5(8)	C(91)−Si(4)−Si(3)	113.8(8)	C(7)−Si(2)−Pt(3)	109.4(4)
extra-ring angles around Pt	P(3)−Pt(1)−P(4)	107.1(2)	P(6)−Pt(3)−P(5)	106.4(2)	P(1)−Pt(1)−Si(2)	99.21(13)
	P(1)−Pt(2)−P(2)	106.7(2)	P(7)−Pt(4)−P(8)	105.7(2)	P(2)−Pt(2)−Si(1)	100.29(13)
					P(1)−Pt(1)−Si(1)	148.55(12)
					P(2)−Pt(2)−Si(2)	148.04(12)

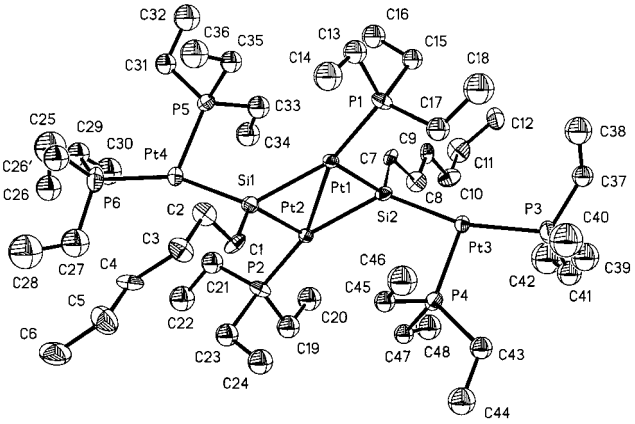

Figure 2. Thermal ellipsoid plot of the crystal structure of **2a** drawn with 50% probability ellipsoids. Hydrogen atoms are omitted for clarity.

Table 3. Selected Bond Lengths (Å) and Angles (deg) for the Pendant Platinum Moieties of 2a

bond lengths		bond angles	
Pt(3)−P(4)	2.279(4)	P(4)−Pt(3)−P(3)	103.37(14)
Pt(3)−P(3)	2.306(4)	P(5)−Pt(4)−P(6)	107.26(15)
Pt(4)−P(5)	2.280(4)	P(3)−Pt(3)−Si(2)	160.72(14)
Pt(4)−P(6)	2.304(4)	P(6)−Pt(4)−Si(1)	157.16(15)
Pt(3)−Si(2)	2.375(4)	P(5)−Pt(4)−Si(1)	95.57(13)
Pt(4)−Si(1)	2.377(4)	P(4)−Pt(3)−Si(2)	95.04(13)

and silicon atoms (P(1)−Pt(1)−Si(1) = 148.55(12)° and P(2)−Pt(2)−Si(2) = 148.04(12)°) are also consistent with the presence of bridging hydrides between these atoms. The exocyclic nonring platinum atoms (Pt(3) and Pt(4)) show a distorted square planar geometry. The large angles between the silicon and a phosphorus atom on the exocyclic platinum atoms (P(3)−Pt(3)−Si(2) = 160.72(14)° and P(6)−Pt(4)−Si(1) = 157.16(15)°) also suggest that a terminal hydride could reside between these atoms. The largest residual features on the final difference map were in positions consistent with both the agostic and the terminal hydrides, but these atoms were not refined. Spectral data supporting the presence of the agostic and terminal hydrides are given below. The core $(Pt-Si)_2$ ring of **2a** is similar in structure to those in $[Pt(PCy_3)(\mu\text{-}H-SiMe_2)]_2$ and $[Pt(PPh_3)(\mu\text{-}H-SiH(IMP))]_2$ (IMP = 2-isopropyl-6-methylphenyl) and to the $(Pd-Si)_2$ ring in $[Pd(PMe_3)(\mu\text{-}H-SiPh_2)]_2$.[6,10,14] These three rings also have alternating metal−silicon bond lengths, acute M−Si−M angles (69.5(3)°, 69.26(3)°, and 69.61(5)°, respectively) and bonding metal−metal distances. The Pt−Si distances of $[Pt(PCy_3)(\mu\text{-}H-SiMe_2)]_2$ (2.324(2) and 2.420(2) Å) and $[Pt(PPh_3)(\mu\text{-}H-SiH(IMP))]_2$ (2.3248(9) and 2.4280(9) Å) are slightly shorter than those in **2a**, whereas the Pt−Pt distances (2.708(1) and 2.7021(2) Å) are slightly longer than that of **2a**.

It is clear that the platinum−silicon frameworks of the rings of **1b** and **2a** are very different; almost the reverse of one another. This converse relationship of **1b** and **2a** is especially evident when Pt−Pt and Si−Si separations and Pt−Si−Pt and Si−Pt−Si angles are compared. Figure 3 compares the heavy atom framework of ***trans*-1b** and **2a**. Interestingly, the average platinum−silicon bond distance within the $(Pt-Si)_2$ rings of both ***trans*-1b** and **2a** is experimentally identical (2.392 vs 2.393 Å).

Infrared Spectral Characterization. The rings **1a**, **1b**, and **2a** were characterized by infrared spectroscopy. The silicon hydrides of **1a** and **1b** were observed at 1985 and 1984 cm^{-1}, respectively. The agostic hydride of **2a** was observed as a broad weak feature at ∼1630 cm^{-1}. In general, a reduction of the stretching frequency is expected when comparing a terminal silicon-hydride to an agostic one.[1a,37] The value of the stretching frequency for the agostic Pt−H−Si of **2a** is similar to those of $[Pt(PR'_3)((\mu\text{-}H)SiR_2)]_2$ (1618−1655 cm^{-1}).[6,10] The terminal

(37) Takao, T.; Yoshida, S.; Suzuki, H.; Tanaka, M. *Organometallics* **1995**, *14*, 3855−3868.

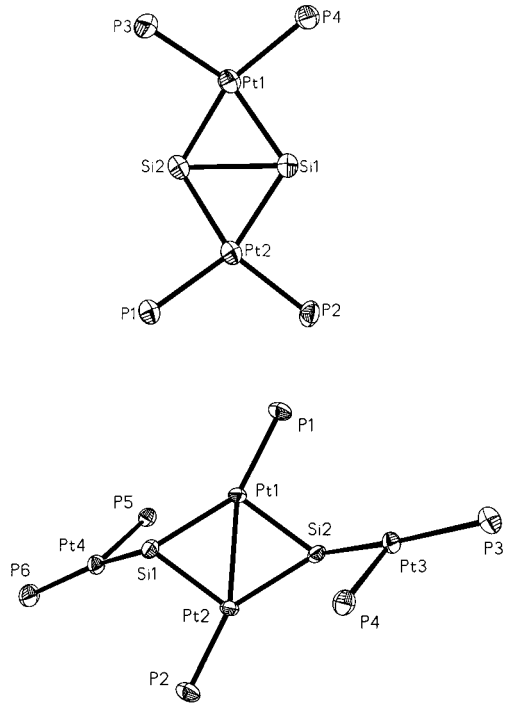

Figure 3. Comparison of the heavy-atom framework for **1b** and **2a**.

platinum-hydride of **2a** was observed as a medium-intensity band at ~2006 cm^{-1}.

NMR Spectral Characterization. The use of routine NMR techniques to characterize the four-membered rings proved insufficient. The agostic hydrides of **2a** could not be located by lD ^1H NMR (see below). Also, the presence of both the ^{31}P and ^{195}Pt nuclei complicated the ^1H and ^{29}Si 1D spectra, from which it was difficult to make accurate assignments of coupling constants. For these reasons a detailed study of the 1D- and 2D[38]-NMR spectra of **1b** and **2a** was undertaken on a 600 MHz instrument. For both **1b** and **2a**, NMR samples were made from the same batch of crystals used for the X-ray crystallographic studies. To simplify the description of the spectra, the numbering system used in the crystal structures of **1b** and **2a** is used to specify their coupling constants.

1D ^{195}Pt NMR Spectra. The 1D ^{195}Pt NMR of spectra of **1b** and **2a**, acquired at 64 MHz, were not only useful in characterizing these compounds but also useful in showing the impurities in the samples. The ^{195}Pt chemical shift of **1b** is −4777 ppm and is observed as a triplet of triplets. In this sample of **1b** the ^{195}Pt signal from a trace amount of **2b** was detected at about −4950 ppm (ring Pt atoms).[39] The coupling pattern and the width of the signal for **2b** resembles that of **1b** but were not well enough resolved to report values for the coupling constants. The spectra of all recrystallized samples of **1b** show weak signals for $Pt(PPr_3)_3$ as well as several very broad multiplets in the range −5450 to −5660 ppm, which are assigned to the decomposition products of $H_2Pt(PPr_3)_n$ ($n = 2, 3$). The ^{195}Pt chemical shift of the ring platinum atoms of **2a** (Pt(1) or Pt(2)) is −4944 ppm. The absorption of the exocyclic platinum atoms of **2a** (Pt(3) or Pt(4)) is observed as a broad multiplet at ~−5500 to −5650 ppm. The spectrum of **2a** also shows several broad multiplets at ~−5300 to −5900 ppm, under the signal for the exocyclic platinum atoms, which are assigned to the decomposition products of $H_2Pt(PEt_3)_n$ ($n = 2, 3$). The coupling to ^{31}P atoms in the 1D ^{195}Pt NMR spectra of **1b** and **2a** will be discussed with the 2D spectra.

1D ^{31}P NMR Spectra. The ^{31}P NMR spectra of **1a** and **1b** show a distinctive pattern for the ^{195}Pt and ^{31}P couplings similar to that described by Braddock-Wilking.[10] The ^{31}P NMR spectrum of **2a** is complex because it displays the overlapping coupling patterns of three inequivalent phosphines. From the platinum−phosphorus coupling (2465 Hz) in the $^{195}Pt-^1H$ 2D-NMR of **2a** (see below) it was possible to assign the ^{31}P resonance for the phosphine (P(1)) that is bonded to the ring platinum (Pt(1)). The remaining two ^{31}P resonances exhibit significantly different platinum−phosphorus couplings. In accord with previous work on $(R_3P)_2PtH(SiR_3)$ complexes,[42] the resonance with the larger platinum−phosphorus coupling (2380 Hz) is assigned to the phosphine trans to the hydride (P(4)), and that with the smaller coupling (1340 Hz) is assigned to the phosphine trans to the silane (P(3)). None of the ^{31}P NMR spectra were sufficiently resolved to extract platinum−platinum couplings for the ring platinum atoms.

2D-NMR Spectra of 1b. The 1D ^1H NMR spectra of **1b** were acquired both with and without ^{31}P decoupling. These spectra show the presence of both trans and cis forms of **1b**. The proton resonance of the silicon hydride in ***trans*-1b** is at 3.89 ppm. This resonance is an apparent heptet from coupling to ^{31}P and ^{195}Pt in the spectrum without ^{31}P decoupling, and a singlet with two satellites from ^{195}Pt coupling (integration about 1:3:1) in the spectrum with ^{31}P decoupling. The signal of the silicon hydride in ***cis*-1b** is at 3.55 ppm and exhibits the same splitting patterns as those of ***trans*-1b**. In this particular sample of **1b**, the ratio of trans to cis isomers is about 15:1. The two-bond H−Pt coupling constant of **1b** ($^2J_{H-Pt}$ = 27 Hz) can be resolved from the 1D ^1H NMR spectra with ^{31}P decoupling. By comparison of both spectra, the three-bond H−P coupling constant of 14 Hz can be obtained.

Figure 4 shows the 2D plot of a section from the long-range $^1H-^{195}Pt$ gradient HMQC[32,39] NMR spectrum of **1b**, which contains correlations between the silicon hydride proton and the ring platinum atoms.

(38) (a) Martin, G. E.; Zektzer, A. S. *Two-Dimensional NMR Methods for Establishing Molecular Connectivity*; VCH: New York, 1988; pp 213−221. (b) *Advanced Applications of NMR to Organometallic Chemistry*; Gielen, M., Willem, R., Wrackmeyer, B., Eds.; John Wiley & Sons: New York, 1996.

(39) The ^{29}Si NMR spectra of **2b** could not be observed because of the low natural abundance of this nucleus.

(40) The ^{195}Pt atom is roughly 1/3 abundant (33.83%), with other platinum isotopes, mostly ^{194}Pt, ^{196}Pt, and ^{198}Pt, being NMR silent. Therefore there are three possible situations for a ring that contains two platinum atoms; both platinum atoms are NMR silent at 4/9 probability, one platinum atom is ^{195}Pt and the other is NMR silent at 4/9 probability, and both platinum atoms are ^{195}Pt at 1/9 probability. The latter situation was not observed due to its low probability.

(41) (a) Schubert, U. *Adv. Organomet. Chem.* **1990**, *30*, 151−187. (b) Corey, J. Y.; Braddock-Wilking, J. *Main Group Chem. News* **1996**, *4*, 6−17. (c) Schneider, J. J. *Angew. Chem., Int. Ed. Engl.* **1996**, *35*, 1069−1075.

(42) Examples with alkyl phosphines: (a) Paonessa, R. S.; Prignano, A. L.; Trogler, W. C. *Organometallics* **1985**, *4*, 647−657. (b) Packett, D. L.; Syed, A.; Trogler, W. C. *Organometallics* **1988**, *7*, 159−166. (c) Mullica, D. F.; Sappenfield, E. L. *Polyhedron* **1991**, *10*, 867−872. (d) Latif, L. A.; Eaborn, C.; Pidcock, A. P. *J. Organomet. Chem.* **1994**, *474*, 217−221. (e) Koizumi, T.; Osakada, K.; Yamamoto, T. *Organometallics* **1997**, *16*, 6014−6015.

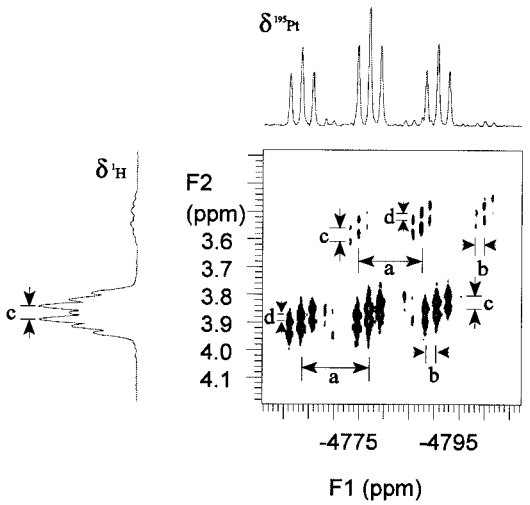

Figure 4. H−Pt gradient HMQC 2D-NMR of **1b** with projections of the 2D spectrum in the ^{195}Pt and ^{1}H dimensions plotted along the horizontal (δ^{195}Pt) and vertical (δ^{1}H) axes, respectively. The $^{2}J_{HPt}$ coupling (labeled **c**) is observed in the projection and is comparable in magnitude to the numerous J_{HP} couplings. This coupling is not resolved in any of the 1D spectra because the 2D experiment selectively detects signals from ^{1}H coupled to ^{195}Pt.

Two sets of triplet of triplet cross-peaks can be observed from the 2D spectrum. The more intense set of cross-peaks is assigned as ^{1}H−^{195}Pt cross-peaks from ***trans*-1b**, and the weaker set of cross-peaks are attributed to ***cis*-1b**. The larger triplet splitting ($^{1}J_{PtP}$ = 1744 Hz, marked **a** in Figure 4) in the ^{195}Pt dimension is due to the two ^{31}P atoms (P(1) and P(2)) bonded directly to ^{195}Pt (Pt(2)). Furthermore, the two ^{31}P atoms (P(3) and P(4)) three bonds away from the ^{195}Pt (Pt(2)) split each triplet into another triplet with a smaller coupling constant ($^{3}J_{PtP}$ = 280 Hz, marked **b** in Figure 4). In the ^{1}H dimension, the silicon-hydride resonance is also split by ^{195}Pt ($^{2}J_{H\ Pt}$ = 27 Hz, marked as **c** in Figure 4) and ^{31}P ($^{3}J_{HP}$ = 14 Hz, marked as **d** in Figure 4) atoms. Exactly the same pattern is observed for the cross-peaks of ***cis*-1b**. The ^{195}Pt chemical shifts of ***trans*-1b** is −4777 ppm, and the ^{1}H chemical shifts of the silicon hydride is 3.87 ppm (there is a small isotope shift compared to the shift from the 1D ^{1}H spectrum). The ^{195}Pt chemical shifts of ***cis*-1b** is −4787 ppm, and the ^{1}H chemical shift of the silicon-hydride is 3.53 ppm.

Figure 5 contains the 2D plots of the ^{1}H−^{29}Si gradient HMQC NMR spectra with ^{29}Si decoupling (Figure 5a) and without ^{29}Si decoupling (Figure 5b) of **1b**.

In Figure 5a, the apparent triplet of triplets pattern, along the ^{29}Si dimension, is due to ^{195}Pt and ^{31}P couplings. The^{195}Pt coupled ^{29}Si signal is expected to be a five-line signal with relative intensities 0.029:0.224: 0.495:0.224:0.029. The ^{29}Si spectrum of **1b** is an apparent triplet of triplets of triplets; the two outside signals of the five-line ^{195}Pt coupling are apparently too weak to be observed. The large splitting (**e**) is from coupling between ^{195}Pt (Pt(1) or Pt(2)) and ^{29}Si (Si(1) or Si(2)), which splits the resonances with $^{1}J_{SiPt}$ = 661 Hz. Each of these lines is further coupled to two ^{31}P atoms (P(2) and P(4), or P(1) and P(3)), resulting in a triplet ($^{3}J_{SiP}$ = 97 Hz, marked as **g** and $^{3}J_{SiP}$ = 48 Hz, marked as **h**). The additional splitting in the center group of peaks is from the ^{29}Si attached to the more abundant, NMR-silent Pt atoms. This splitting shows both types of three-bond ^{29}Si and ^{31}P couplings (**g** and **h**). Similarly, in the proton dimension, the three-bond ^{1}H−^{31}P coupling (**d**) and two-bond ^{1}H−^{195}Pt coupling (**c**) are also observed as in Figure 4. In Figure 5b, without ^{29}Si decoupling, all of the above couplings are seen in addition to the ^{1}H−^{29}Si one-bond coupling ($^{1}J_{HSi}$ = 160 Hz, marked as **f** in Figure 5b). The ^{29}Si and ^{1}H chemical shifts of the silicon hydride in ***trans*-1b** are −92.30 and 3.89 ppm, respectively. The ^{1}H−^{29}Si HMQC 2D NMR spectrum without ^{31}P decoupling also exhibits weak cross-peaks from the silicon hydride in ***cis*-1b**. This silicon-hydride has a ^{29}Si chemical shift of −72.96 ppm and ^{1}H chemical shift of 3.55 ppm. The ^{1}H chemical shifts of both isomers are similar to those obtained from the 1D ^{1}H NMR experiment.

2D-NMR Spectra of 2a. The 1D ^{1}H NMR spectra of **2a** were acquired both with and without ^{31}P decoupling. The proton resonance of the terminal platinum hydride (H−Pt(3) or H−Pt(4)) of **2a** was observed as a singlet at −2.29 ppm, with a satellite doublet due to ^{195}Pt coupling ($^{1}J_{HPt}$ = 995 Hz). Without ^{31}P decoupling, each peak of the triplet mentioned above is split into a doublet of doublets, which is due to the two types of two-bond ^{1}H−^{31}P couplings ($^{2}J_{HP(trans)}$ = 150 Hz, and $^{2}J_{HP(cis)}$ = 25 Hz). The ^{1}H signal from the agostic hydride of **2a** cannot be resolved because it overlaps with the signals of the aliphatic protons. In contrast to **1b**, there is no evidence for a second isomer of **2a** in the NMR spectra, and therefore it is assumed that the species in solution has the same trans arrangement (relative to the Si−Si vector) of the hexyl and exocyclic platinum substituents as in the crystal structure.

Because of the better dispersion in the 2D-NMR experiment, both ^{1}H−^{195}Pt and ^{1}H−^{29}Si correlations of the agostic hydride of **2a** have been detected via 2D gradient HMQC experiments. A separate 2D experiment to correlate ^{1}H and exocyclic ^{195}Pt shifts was not possible because the long-range coupling ($^{2}J_{HPt}$) between these atoms was not resolved. Therefore, only the cross-peak from the agostic ^{1}H−^{195}Pt correlation has been observed in the 2D ^{1}H−^{195}Pt plot of **2a** (Figure 6).

For the two ring platinum atoms (Pt(1) and Pt(2)) of **2a** the most likely situation that will give ^{195}Pt coupling is that one platinum is ^{195}Pt and that the other is NMR silent.[40] For this discussion we assign Pt(1) to ^{195}Pt. Both ^{1}H−^{195}Pt and ^{1}H−Pt−^{195}Pt correlations can be detected in the 2D experiment. Protons attached to NMR-silent platinum atoms have slightly different chemical shifts compared with those protons attached to ^{195}Pt. For the ^{1}H−^{195}Pt correlation of **2a**, the ^{31}P (P(1)) directly attached to Pt(1) splits the ^{195}Pt resonance into a large doublet ($^{1}J_{PtP}$ = 2465 Hz, marked as **i** in Figure 6) along the ^{195}Pt dimension; it also splits the pattern in the ^{1}H dimension (H−Pt(1)) into a doublet ($^{2}J_{HP}$ = 15 Hz, marked as **k**). Concurrently, the second ^{31}P (P(2)) two bonds away from ^{195}Pt (Pt(1)) can split each ^{195}Pt peak into another doublet ($^{2}J_{PtP}$ = 1346 Hz, marked as **j**); however, the coupling between this ^{31}P (P(2)) and the agostic proton (H−Pt(1)) is very weak and cannot be resolved in the 2D spectrum. Therefore, the cross-peak from the ^{1}H−^{195}Pt correlation of **2a** shows a doublet with small splitting aligned along the ^{1}H dimension and a doublet with large splitting tilted from the ^{1}H dimen-

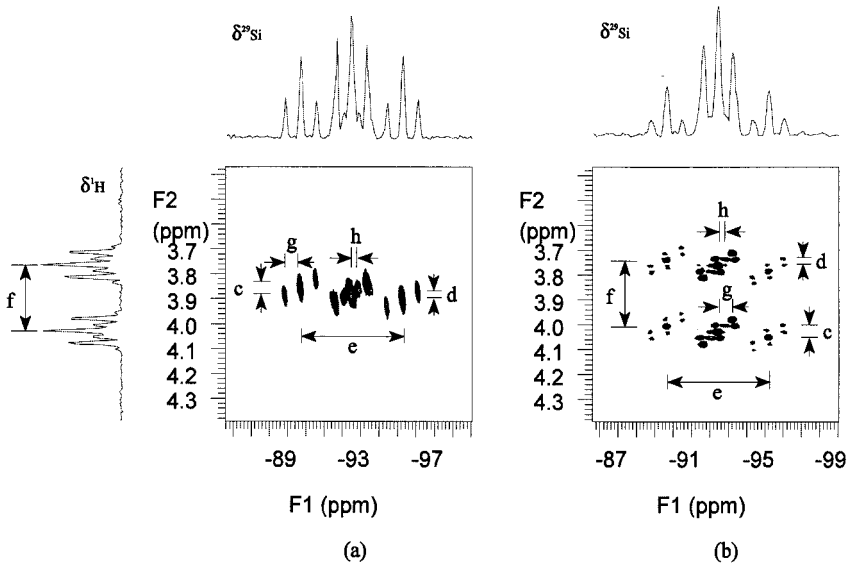

Figure 5. H−Si gradient HMQC 2D-NMR of **1b**: (a) with ^{29}Si decoupling during the acquisition period and (b) without ^{29}Si decoupling during the acquisition period. Projections of the 2D spectrum (b) in the ^{29}Si and ^{1}H dimensions are plotted along the horizontal and vertical axes, respectively. The large separation between the two multiplets in the ^{1}H projection (labeled **f**) is $^{1}J_{HSi}$. This splitting pattern is clearly observed in the 2D projection and not seen in the 1D spectrum because the 2D experiment selectively detects signal from ^{1}H bound to ^{29}Si.

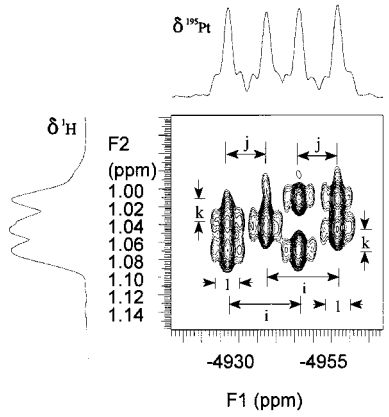

Figure 6. H−Pt gradient HMQC 2D-NMR of **2a** with projections of the 2D spectrum in the ^{195}Pt and ^{1}H dimensions plotted along the horizontal (δ^{195}Pt) and vertical (δ^{1}H) axes, respectively.

sion. For the ^{1}H−Pt−^{195}Pt correlation, the ^{31}P (P(1)) directly attached to ^{195}Pt (Pt(1)) splits the ^{195}Pt resonance into a large doublet ($^{1}J_{PtP}$ = 2465 Hz, marked as **i** in Figure 6) along the ^{195}Pt dimension; however, the coupling between this ^{31}P (P(1)) and the agostic proton (H−Pt(2)) is very weak and cannot be resolved in the 2D spectrum. At the same time, another ^{31}P (P(2)) two bonds away from ^{195}Pt (Pt(1)) can split each ^{195}Pt peak into another doublet (doublet of doublet) ($^{2}J_{PtP}$ = 1346 Hz, marked as **j**) and also splits the ^{1}H (H−Pt(2)) into a doublet ($^{2}J_{HP}$ = 15 Hz, marked as **k**). In this way, the cross-peak from the ^{1}H−Pt−^{195}Pt correlation of **2a** displays a doublet with the large horizontal splitting and a doublet with small splitting tilted from the ^{1}H dimension. The ^{1}H chemical shift for ^{1}H−^{195}Pt correlation is 1.03 ppm. The ^{1}H chemical shift for ^{1}H−Pt−^{195}Pt correlation of **2a** is 1.05 ppm. Both ^{195}Pt chemical shifts (δ^{195}Pt = 1325.6 ppm) are identical (within the resolution of the spectrum). Further splitting by an exocyclic ^{195}Pt atom (Pt(3) or Pt(4), $^{2}J_{PtPt}$ = 1644 Hz, marked as **l**) on each cross-peak is observed in the 2D spectrum.

Because of the low concentration of the sample, the ^{1}H−^{29}Si 2D gradient HMQC experiment of **2a** mainly detects signals from the correlations between ^{1}H and ^{29}Si attached to NMR-silent platinum atoms; the signals from ^{1}H−^{29}Si−^{195}Pt are undetectable. However, the correlation from the agostic bond ^{195}Pt−^{1}H−^{29}Si was observed in the 2D experiments, and the ^{1}H (δ^{1}H = 1.03) and ^{29}Si (δ^{29}Si = 194.68) chemical shifts of **2a** were obtained from the cross-peaks (Figure 7).

Figure 7a shows the 2D plot of the ^{1}H−^{29}Si gradient HMQC with ^{29}Si decoupling of **2a**. The doublet of doublet pattern along the ^{29}Si dimension is observed, which is due to coupling with two different ^{31}P atoms which are two bonds away ($^{2}J_{SiP(trans)}$ = 132 Hz, marked as **m**; and $^{2}J_{SiP(trans)}$ = 95 Hz, marked as **n)**. It was not possible to distinguish which ^{31}P atom causes the larger splitting in **2a**. Along the ^{1}H dimension, the two-bond H−Pt(1)−P(1) coupling constant can be resolved ($^{2}J_{HP(cis)}$ = 15 Hz, marked as **p**) and is the same as that (marked as **k**) observed in Figure 6. Figure 7b shows the 2D ^{1}H−^{29}Si gradient HMQC obtained without ^{29}Si decoupling of **2a**. All the information obtained from Figure 7a can be seen here, plus the one-bond (agostic) ^{1}H−^{29}Si coupling ($^{1}J_{HSi(agostic)}$ = 30 Hz, marked as **q** in Figure 7b). In the 2D-NMR spectrum of **2a**, the very weak ^{195}Pt satellite peaks ($^{1}J_{SiPt}$ = 707 Hz) were barely observed above the noise level along the ^{29}Si dimension (not shown in Figure 7).

Discussion of the NMR Spectra. Chemical shift and coupling information from the NMR study of **1b** and **2a** are listed in Table 4.

We note that the chemical shift and coupling values in Table 4 may differ slightly from those in the Experimental Section for a number of reasons. The results reported in Table 4 were obtained on a higher resolution instrument (300 vs 600 MHz) than those reported in

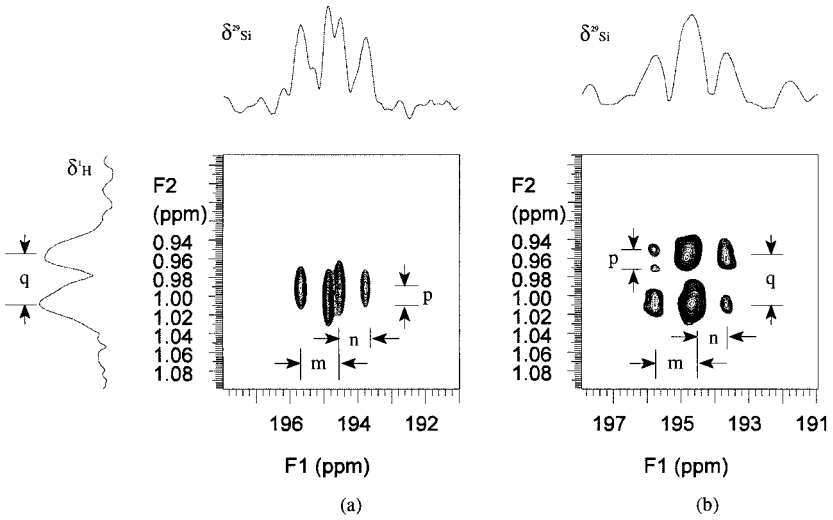

Figure 7. H−Si gradient HMQC 2D-NMR of **2a**: (a) with ^{29}Si decoupling during the acquisition period and (b) without ^{29}Si decoupling during the acquisition period. Projections of the 2D spectrum (b) in the ^{29}Si and ^{1}H dimensions are plotted along the horizontal and vertical axes, respectively. The large separation between the two multiplets in the ^{1}H projection (labeled **q**) is $^{1}J_{HSi}$. This splitting is different in the 1D spectrum, as the 2D experiment selectively detects signal from ^{1}H bound to ^{29}Si, while the signals in the 1D spectrum are from ^{1}H bound to ^{28}Si.

Table 4. Chemical Shifts and Coupling Constants of 1b and 2a[a]

	compound **1b**		
	***trans*-1b**	***cis*-1b**	compound **2a**
δ ^{1}H (ppm)	3.89 (**H**-Si(1))	3.55 (**H**-Si)	1.03−1.05 (agostic Si(1)−**H**−Pt(1)) −2.29 (terminal **H**−Pt(3))
δ ^{195}Pt (ppm)	−4777	−4787	−4944 (agostic Si(1)−H−**Pt**(1)) −5500 to −5650 (pendant **Pt**(3)−H)
δ ^{29}Si (ppm)	−92.30	−72.96	194.68
$^{1}J_{HSi}$ (Hz)	160 (**f**, **Si**(1)−**H**)	160 (**f**)	30 (**q**, Si(1)−agostic H)
$^{1}J_{HPt}$ (Hz)			995 (terminal **H**−**Pt**(3)) not observed (agostic Si(1)−**H**−**Pt**(1))
$^{2}J_{HPt}$ (Hz)	27 (**c**, **H**−Si(1)−**Pt**(1))	27 (**c**)	
$^{2}J_{HP}$ (Hz)			150 (**H**−Pt(3)−**P**(4)) 25 (**H**−Pt(3)−**P**(3)) 15 (**k**, **H**−Pt(1)−**P**(1))
$^{3}J_{HP}$ (Hz)	14 (**d**) (**H**−Si(1)−Pt(2)−**P**(2))	14 (**d**)	not observed
$^{1}J_{PtP}$ (Hz)	1744 (**a**) (**Pt**(1)−**P**(3))	1744 (**a**)	2465 (**i**, **Pt**(1)−**P**(1))
$^{2}J_{PtP}$ (Hz)			1346 (**j**, **Pt**(1)−Pt(2)−**P**(2))
$^{3}J_{PtP}$ (Hz)	280 (**b**) (**Pt**(1)−Si(1)−Pt(2)−**P**(1))	280 (**b**)	not observed
$^{1}J_{SiPt}$ (Hz)	661 (**e**) (**Si**(1)−**Pt**(1))	661 (**e**)	707 (**Si**(1)−**Pt**(1))
$^{2}J_{SiP}$ (Hz)	97 (**g**, **Si**(1)−Pt(2)−**P**(1)) 48 (**h**, **Si**(1)−Pt(2)−**P**(2))	97 (**g**) 48 (**h**)	132 (**m**), 95 (**n**) (either **Si**(1)−Pt(1)−**P**(1) or **Si**(2)−Pt(3)−**P**(3))
$^{2}J_{PtPt}$ (Hz)			1644 (**l**, **Pt**(1)−Si(2)−**Pt**(3))

[a] Coupling constants are specified using the atomic numbering system from the crystal structures.

the Experimental Section. The ^{31}P decoupling used for the 1D 600 MHz ^{1}H spectra permitted better determination of the coupling constants with respect to those extracted from the routine 300 MHz spectra. Also, the 2D experiments give chemical shifts for protons bound only to ^{29}Si and ^{195}Pt, whereas the 1D spectra give the shifts for protons bound primarily to ^{28}Si and the other platinum nuclei. Slight differences in such isotope

chemical shifts are expected. The use of external referencing for the ^{29}Si, ^{31}P, and ^{195}Pt NMR spectra also introduces slight errors.

Even though **1a** was not one of the subjects of the in-depth NMR study, it is clear that NMR parameters for **1a** resemble those of **1b**. The ^{29}Si chemical shifts of the trans isomers of **1a** and **1b** differ by 1 ppm, and the chemical shifts of the cis isomers differ by 7 ppm. The coupling constants of **1a**, as far as they were determined, are similar to those of **1b**. For both **1a** and **1b**, the chemical shifts of the platinum, silicon, and the hydride atoms of the trans and cis isomers differ, but the coupling constants exhibited by the two isomers are identical. Similar observations can be made with respect to the NMR parameters of $[Pt(PEt_3)_2(\mu\text{-SiXR})]_2$ and the recently reported $[Pt(PPhMe_2)_2(\mu\text{-SiH(IMP)})]_2$ in comparison to those of **1a** or **1b**; the coupling constants are more similar than are the chemical shifts.[10,11]

The coupling constants and chemical shifts of **1b** and **2a** have provided useful structural information. The value of the chemical shift for the agostic proton of **2a** is similar to that of $[Pt(PPh_3)(\mu\text{-H}-\text{SiH(IMP)})]_2$ (2.17 ppm) and to that of the agostic deuteride in the complex $[Pt(PMe(t\text{-}Bu)_2)(\mu\text{-D-SiMe}_2)]_2$ (1.87 ppm).[6,10] The values of the ^{1}H−^{29}Si coupling constant for **1b** (160 Hz) and **2a** (30 Hz) are consistent with a terminal (Pt(3)−H or Pt(4)−H) and agostic hydride (Pt(1)−H−Si(1) or Pt(2)−H−Si(2)), respectively.[1a,41] The value of the coupling constant for the agostic hydride of **2a** is toward the lower end of the expected range (∼20−80 Hz). For this reason, a significant ^{195}Pt−^{1}H coupling constant for the agostic hydride in **2a** was expected, but none was observed. The value of the ^{195}Pt−^{1}H coupling constant for the terminal hydride of **2a** is similar to those found in other square planar $Pt(H)(SiR_3)(PR'_3)_2$ compounds (858−972 Hz).[42] The significant two-bond coupling between the exocyclic ^{195}Pt atom (Pt(3) or Pt(4)) and a ring ^{195}Pt atom of **2b** (Pt(1) or Pt(2)) is unusual.[43] Such a large splitting is usually an indication of a direct Pt−Pt bond. Comparable Pt−Pt couplings in other Pt−X−Pt systems (X = sulfur or phosphorus moiety or halogen or hydride atom) are in the range 125−962 Hz, and in some cases, the couplings are negative. An exception to this pattern is the $^2J_{Pt-Pt}$ value of **3**, which is 3073 Hz.[8] Because of the quality of the ^{31}P NMR spectra, we could not obtain $^2J_{Pt-Pt}$ for the two ring platinum atoms of either **1b** or **2a**. In themselves, the values for $^1J_{Pt-P}$ of **1b** and **2a** do not help to determine the oxidation state at the platinum because the ranges for Pt(0) and Pt(II) complexes are ∼60−9000 Hz and 1400−5000 Hz, respectively.[43,44] For comparison, other rings of structure **1** show Pt−P couplings of roughly 1330−1800 Hz, a similar range of Pt−P coupling constants (∼1150−1890 Hz) is observed for *cis*-$Pt(SiR_3)_2(PR'_3)_2$ complexes, the disilene complexes $Pt(R_2SiSiR_2)(PR_3)_2$ show a wider range of Pt−P coupling constants (1370−2730 Hz), and the lower valent platinum of **3** shows a Pt−P coupling of 2013 Hz.[5b−d,7,9−11,45] Surprisingly, even though the structures of their core $(Pt-Si)_2$ rings are similar, the platinum−phosphorus coupling constants of $[Pt(PPh_3)(\mu\text{-H}-\text{SiH(IMP)})]_2$ and $[Pt(PCy_3)(\mu\text{-H}-\text{SiMe}_2)]_2$ and related rings are in the range 3980−4276 Hz, whereas that for **2a** is 2465 Hz.[6] The Pt−Si coupling constants of **1a** and **2b** are similar. For comparison the Pt−Si coupling constants are somewhat smaller than those reported for *cis*-P_2PtSi_2 complexes (928−1411 Hz) systems and similar to those of the lower valent platinum in **3** (771 Hz).[8]

The most pronounced difference in the NMR spectra of compounds of structures **1** and **2** is their ^{29}Si chemical shifts, which differ by over 250 ppm. It is remarkable that the differing number and arrangement of platinum atoms and phosphine and hydride ligands can alter the chemical shift of the silicon so dramatically. A similarly large difference in chemical shifts has been observed for the rings $[Pt(PPhMe_2)_2(\mu\text{-SiH(IMP)})]_2$ (trans = 131 ppm, cis = 126 ppm) and $[Pt(PPh_3)(\mu\text{-H}-\text{SiH(IMP)})]_2$ (−134 ppm).[10] The chemical shift of **2a** occurs in a region that is usually associated with low-valent silicon compounds such as silylenes, metal−silylenes, and silicenium ions.[46−48] Particularly pertinent examples are the ^{29}Si chemical shifts of the platinum silylene complexes $((i\text{-}Pr)_3P)_2Pt{=}SiMes_2$ and $(Cy_3P)_2Pt{=}SiMes_2$ (Mes = mesityl), which exhibit resonances at +358 and +368 ppm, respectively, and which could be viewed as analogues of the monomers of **1**. The chemical shifts of both the trans or the cis isomers of **1a** and **1b** occur in a region that is associated with tetravalent or hypervalent silicon compounds.[46] These chemical shifts are at least 420 ppm different than those of the platinum−silylenes. As shown in a recent review, the ^{29}Si chemical shift of most bridging silylene complexes, including complexes with agostic M−H−Si moieties, occur in the range +60 to +290 ppm.[3] Therefore, even though exocyclic platinum moieties are present, the ^{29}Si chemical shift of **2a** is in the expected range. The negative ^{29}Si chemical shifts of **1a**, **1b**, $[Pt(PEt_3)_2(\mu\text{-SiXR})]_2$, and $[Pt(PPhMe_2)_2(\mu\text{-SiH(IMP)})]_2$ are unusual, and this would be consistent with the unusual bonding descriptions attributed to

(43) (a) Pregosin, P. S. *Ann. Rep. NMR Spectrosc.* **1986**, *17*, 285−349. (b) Goodfellow, R. J. In *Multinuclear NMR*; Mason, J., Ed.; Plenum: New York, 1987; Chapter 20. (c) Pregosin, P. S. In *Transition Metal Nuclear Magnetic Resonance*; Pregosin, P. S., Ed.; Elsevier: New York, 1991; pp 216−263.

(44) (a) Pregosin, P. S.; Kunz, R. W. *^{31}P and ^{13}C NMR of Transition Metal Complexes*; Springer-Verlag: New York, 1979. (b) Pregosin, P. S. In *Phosphorus-31 NMR Spectroscopy in Stereochemical Analysis*; Verkade, J. G., Quin, L. D., Eds.; VCH: New York, 1987; Chapter 14. (c) Verkade, J. G.; Mosbo, J. A. In *Ibid.*; Chapter 13.

(45) (a) Yamashita, H.; Kobayashi, T.; Hayashi, T.; Tanaka, M. *Chem. Lett.* **1990**, 1447−1450. (b) Schubert, U.; Müller, C. *J. Organomet. Chem.* **1991**, *418*, C6 − C8. (c) Yamashita, H.; Tanaka, M.; Goto, M. *Organometallics* **1992**, *11*, 3227−3232. (d) Gossage, R. A.; McLennan, G. D.; Stobart, S. R. *Inorg. Chem.* **1996**, *35*, 1729−1732. (e) Gilges, H.; Kickelbick, G.; Schubert, U. *J. Organomet. Chem.* **1997**, *548*, 57−63. (f) Tsuji, Y.; Nishiyama, K.; Hori, S.: Ebihara, M.; Kawamura, T. *Organometallics* **1998**, *17*, 507−512. (g) Ozawa, F.; Kamite, J. *Organometallics* **1998**, *17*, 5630−5639.

(46) (a) Kupce, È.; Lukevics, E. In *Isotopes in the Physical and Biomedical Science*; Buncel, E., Jones, J. R., Eds.; Elsevier: Amsterdam, 1991; Vol. 2, Chapter 5. (b) Williams, E. A. *Ann. Rep. NMR Spectrosc.* **1983**, *15*, 235−289. (c) Marsmann, H. In *NMR Basic Principles and Progress, Oxygen-17 and Silicon-29*; Diehl, P., Fluck, E., Kosfeld, R., Eds.; Spriger-Verlag: New York, 1981; Vol. 17, pp 65−235. (d) Kennedy, J. D.; McFarlane, W. In *Multinuclear NMR*; Mason, J., Ed.; Plenum: New York, 1987; Chapter 11. (e) Takeuchi, Y. In *The Chemistry of Organic Silicon Compounds*, Vol. 2; Rappoport, Z., Apeloig, Y., Eds.; John Wiley & Sons: New York, 1998; Part 1, Chapter 6.

(47) (a) Maerker, C.; Schleyer, P. v. R. In *The Chemistry of Organic Silicon Compounds*, Vol. 2; Rappoport, Z., Apeloig, Y., Eds.; John Wiley & Sons: New York, 1998; Part 1, Chapter 10. (b) Lickiss, P. D. In *Ibid.*; Part 1, Chapter 11. (c) Gaspar, P. P.; West, R. In *Ibid.*; Part 3, Chapter 43.

(48) Mitchell, G. P.; Tilley, T. D. *Angew. Chem., Int. Ed. Engl.* **1998**, *37*, 2524−2526.

(49) Feldman, J. D.; Mitchell, G. P.; Nolte, J.-O.; Tilley, T. D. *J. Am. Chem. Soc.* **1998**, *120*, 11184−11185.

these rings.[10−13] We note that the negative chemical shifts of the silicon atoms within the ring of **3** (−59.94 ppm[8]) are similar to those of the cis isomers of **1a** and **1b**. In contrast, the ^{195}Pt chemical shifts of the ring platinum atoms of **1a** or **1b** appear to be rather similar to those of **2a** considering the wide range of known ^{195}Pt chemical shifts (∼15 000 ppm).[43]

Conclusion

In summary, we have synthesized platinum−silicon rings of structures **1** and **2** by a route in which the rings **1** are precursors to **2**. These rings have been characterized by X-ray crystallography and by 1D- and 2D-NMR studies. The structural and spectral data indicate that the bonding in metal−silicon rings of structure **1** is different than in other metal−silicon rings. The most pronounced spectral differences between rings **1** and **2** are their ^{29}Si NMR chemical shifts and their cross-ring Si−Si and Pt−Pt distances. ^{1}H−^{195}Pt and ^{1}H−^{29}Si 2D HMQC NMR experiments provide sensitive detection, dispersion, and resolution of the extensive heteronuclear coupling network of compounds **1b** and **2a**. The availability of this extra information is an extremely useful aid in the characterization of these structures. This research leaves several questions unanswered, which we will address in future publications. We are interested in studying other interconversions between $(Pt−Si)_2$ rings. We also wonder whether the ^{29}Si NMR chemical shift can be correlated with structure. It would seem reasonable to expect a chemical shift intermediate between that of **1** and **2** for a ring such as **4**.

Acknowledgment. We thank M. Fink, J. Corey, J. Braddock-Wilking, and S. Alvarez for useful discussions. This material is based upon work supported by the National Science Foundation under Grant No. 9708181. The support of this research by the University of Akron is gratefully acknowledged. We thank the Kresge Foundation and the donors to the Kresge Challenge at the University of Akron for the funds used to purchase the 600 MHz spectrometer used in this work. C.T. and W.Y. thank Francois Diederich, Peter Chen, and Hans-Joerg Grutzmacher for hosting sabbatical leaves at ETH-Zürich, during which time this paper was written, and the Swiss National Science Foundation for support. We gratefully acknowledge a loan of platinum reagents from Johnson Matthey.

Supporting Information Available: Tables of crystal data, structure solution and refinement, atomic coordinates, bond lengths and angles, and anisotropic thermal parameters for **1b** and **2a**. This material is available free of charge via the Internet at http://pubs.acs.org.

OM990871L